

Université de Montréal

Experimental and Theoretical Studies on the Conformational Properties of *cis*- and *trans*-4,5-methano-L-prolines

par

Ingrid Chab-Majdalani

Département de chimie

Faculté des arts et des sciences

Mémoire présenté à la Faculté des études supérieures et postdoctorales

en vue de l'obtention du grade de maître ès sciences (M. Sc.) en chimie

March 2016

© Ingrid Chab-Majdalani, 2016

Résumé

Il est connu que les 4,5-méthano-L-prolines ont des conformations et des caractéristiques différentes que la L-proline. L'aplatissement du cycle pyrrolidine dans la proline joue un rôle important dans sa stabilité et la conformation spatiale des analogues 4,5-méthano- de la L-proline. Ainsi, des études approfondies ont été menées pour analyser les différences de structure et les modèles de pliage des *cis*- et *trans*-4,5-méthano-L-prolines et leurs oligomères en corrélation avec la délocalisation électronique $n \rightarrow \pi^*$ entre les carbonyles adjacents. Dans cette thèse, la stabilisation $n \rightarrow \pi^*$ entre les groupes carbonyle d'une amide et un ester a été analysée, divulguant des propriétés structurales supplémentaires des 4,5-méthano-L-prolines. Les études spectroscopiques en RMN ont révélé les caractéristiques spatiales des *cis*- and *trans*-4,5-méthano-L-prolines corrélant avec l'équilibre d'isomérisation de l'amide *trans* : *cis* dans des environnements différents. En outre, le mécanisme de la cyclisation intramoléculaire des dimères *cis-cis*, *trans-trans*, et du mélange *trans,cis*-4,5-méthano-L-proline dans la formation des dicétopipérazines a révélé l'importance de la stabilisation $n \rightarrow \pi^*$ sur les caractéristiques conformationnelles et de pliage. Des études de modélisation DFT ont également été menées afin de compléter nos résultats et de fournir des explications soutenant nos résultats expérimentale.

Mots Clés: méthanoproline, isomérisation *trans* : *cis*, dicétopipérazines.

Abstract

It is well known that 4,5-methano-L-prolines have different conformational properties and characteristics than proline. The flattening of the pyrrolidine ring plays a role in the stability and conformation of L-proline methanologs. Thus, extensive studies have been conducted to analyze the structural differences and folding patterns of *cis*- and *trans*-4,5-methano-L-prolines and their oligomers in correlation with the $n \rightarrow \pi^*$ electron delocalization between the adjacent carbonyls of amide and ester groups. In this thesis, the $n \rightarrow \pi^*$ stabilization of each derivative is analyzed, disclosing additional structural properties of 4,5-methano-L-prolines. NMR spectroscopic studies revealed the spatial characteristics of *cis*- and *trans*-4,5-methano-L-prolines in correlation to the amide *trans* : *cis* isomerization equilibrium in different solvents. In addition, the tendency of diketopiperazine formation from the *cis-cis*, *trans-trans*, and mixed *trans,cis*-4,5-methano-L-proline dimers reflected the importance of the $n \rightarrow \pi^*$ stabilization on the conformation and folding characteristics.

Keywords: methanoproline, polyproline, *trans* : *cis* isomerization, diketopiperazine.

Table of Contents

Abbreviations.....	vi
List of Figures.....	xii
List of Tables.....	xiv
List of Schemes	xiv
Acknowledgements.....	xv

Chapter 1

Introduction.....	1
Importance of Proline Conformation and Polyproline Helices in Proteins.....	1
<i>Cis</i> - and <i>trans</i> -4,5-Methano-L-proline.....	8
Comparisons of the Conformations of Proline and its 4,5-Methano-L-proline Analogs.....	12
Diketopiperazine Formation.....	16

Chapter 2

Results and Discussion	20
Synthesis of <i>cis</i> and <i>trans</i> -4,5-Methano-L-proline.....	20
Electronic Effects on the <i>trans-cis</i> Isomerization Equilibrium.....	24
Kinetic and Conformational Studies of Diketopiperazine Formation.....	31

Chapter 3

Conclusion.....	37
-----------------	----

Chapter 4

Experimental Notes.....	38
Experimental Procedures.....	39
Synthesis of <i>trans</i> -4,5-Methano-L-proline.....	39
Synthesis of <i>cis</i> -4,5-Methano-L-proline.....	44
Synthesis of acetylated derivatives Ac-Pro-OEt, <i>cis</i> -Ac-MP-OEt, and <i>trans</i> -Ac-MP-OEt.....	46
Synthesis of <i>cis-cis</i> , <i>trans-trans</i> , and <i>trans-cis</i> -4,5-methano-L-proline dimers	49
Synthesis of individual diketopiperazines.....	55

Chapter 5

References.....	59
-----------------	----

Abbreviations

Ac acetyl

Ala alanine

Amp 3,4-(aminomethano)proline

ATP adenosine triphosphate

Boc *tert*-Butyloxycarbonyl protecting group

Bu butyl

cat. Catalytic

CD circular dichroism

cis-cis cis-4,5-Methano-L-proline dimer

CRP collagen-related peptides

CSA camphorsulfonic acid

DFT Density Functional Theory

DIPEA *N,N*-diisopropylethylamine

DKP diketopiperazine

DMAP 4-dimethylaminopyridine

DMF dimethylformamide

DMSO- d_6 deuterated dimethyl sulfoxide

DPP-IV dipeptidyl peptidase IV

EDC 1-ethyl-3-(3-dimethylaminopropyl)carbodiimide

Et ethyl

EWG electron-withdrawing group

Flp (2*S*, 4*R*)-4-fluoroproline

g gram

GLP-1 glucagon-like peptide 1

Gly glycine

GPR γ -glutamyl phosphate reductase

h hours

HOBt hydroxybenzotriazole

HRMS high resolution mass spectrometry

Hyp hydroxyproline

LiHMDS lithium bis(trimethylsilyl)amide

M molar

Me methyl

mg milligram

min minute

mL milliliter

mM millimolar

mmol millimol

NAD⁺ nicotinamide adenine dinucleotide (oxidized form)

NADH nicotinamide adenine dinucleotide (reduced form)

NBO natural bond orbital

NMR nuclear magnetic resonance

NOE nuclear Overhauser effect

P5C5S pyrroline-5-carboxylate synthase

P_i monophosphate

PPI polyproline I type helix

PPII polyproline II type helix

ppm parts per million

PPTS pyridinium *p*-toluenesulfonate

Pro L-proline

R alkyl group

RT room temperature

SSF Simmons-Smith-Furukawa

T temperature

TBDPS *tert*-Butyldiphenylsilyl

TEMPO (2,2,6,6-Tetramethylpiperidin-1-yl)oxyl

TFA trifluoroacetic acid

TFAA trifluoroacetic anhydride

THF tetrahydrofuran

TLC thin layer chromatography

trans-cis mixed *trans/cis*-4,5-Methano-L-proline dimer

trans-trans *trans*-4,5-Methano-L-proline dimer

TS transition state

Xaa amino acid X

XRD X-ray diffraction

Yaa amino acid Y

List of Figures

Figure 1. Chemical structure of L-Proline (Pro)

Figure 2. X-Ray crystallography of the collagen triple helix.

Figure 3. *C γ -endo* and *C γ -exo* puckers.

Figure 4. The effect of electron-withdrawing groups on the gauche effect and *C γ* -puckering.

Figure 5. Secondary structures: α -helices and β -sheets.

Figure 6. Crystal structure of polyproline type I (PPI) and polyproline type II (PPII) helices.

Figure 7. *cis*- and *trans*-4,5-Methano-L-prolines.

Figure 8. Inhibitory pathway of DPP-IV on GLP-1.

Figure 9. Early generations of proline-based dipeptidase IV inhibitors.

Figure 10. The eight stereoisomers of Onglyza.

Figure 11. The first crystal structure of proline hexamer *p*-Br-C₆H₄-Pro₆-COOH.

Figure 12. Depiction of $n \rightarrow \pi^*$ interaction and effect of pyramidalization on the proline ring.

Figure 13. Diketopiperazine formation of Ala-Pro-COOEt.

Figure 14. *Cis* : *trans* isomerization of the Ac-Pro-OEt amide bond.

Figure 15. Ac-Pro-OMe and tertiary amide Ac-Pro-NMe₂.

Figure 16. ¹H NMR and 1D NOE spectra of minor and major isomer differentiation of Ac-Pro-OEt.

Figure 17. 1D NOE spectra of Ac-Pro-OEt.

Figure 18. The experimental $K_{trans/cis}$ values obtained for Ac-Pro-OEt, *cis*-Ac-MP-OEt, and *trans*-Ac-MP-OEt.

Figure 19. Cyclization of *cis-cis*-4,5-methano-L-proline to a diketopiperazine

Figure 20. Time-lapse illustration of the starting material peaks disappearing and the diketopiperazine peaks appearing in the ^1H NMR spectrum of the *cis-cis* free amine dimer at 10 min, 7 and 15 days.

Figure 21. Rate of diketopiperazine formation of *pro-pro*, *trans-trans*, *trans-cis*, and *cis-cis*-4,5-methano L-prolines

List of Tables

Table 1. Ring puckering and dihedral angles of the proline hexamer.

List of Schemes

Scheme 1. Biosynthesis of Pro from glutamic acid.

Scheme 2. Diketopiperazine synthetic route of 3,4-(aminomethano)proline.

Scheme 3. The first synthetic procedure to 4,5-methano-L-proline through stannane-based intramolecular carbocyclization.

Scheme 4. Synthesis of *cis*-4,5-methano-L-proline through Simmons-Smith-Furukawa cyclopropanation.

Scheme 5. Synthesis of *trans*-4,5-methano-L-proline using TBDPS as the protecting group,

Scheme 6. General synthetic procedure to the *pro-pro*, *cis-cis*, *trans-trans*, and *trans-cis*-4,5-methano L-proline dimers.

Acknowledgements

Firstly, I would like to thank my research supervisor Professor Stephen Hanessian for accepting me in his research group as a graduate student. He is a Professor of high standards who encouraged me to do my best in my work. I will forever be grateful for all that he has taught me throughout my graduate studies.

I would also like to thank Gilles for his guidance and DFT calculations that he conducted for this project. Moreover, I would like to thank Miguel, Michael, and Oscar who have taken some of their time to help me throughout my studies. Finally, I would like to thank my parents for their unconditional support they have provided me during the whole duration of my studies.

Introduction

Importance of Proline Conformation and the Polyproline Helix in Proteins

Proline **1.1** is one of the twenty amino acids utilized by Nature in the biosynthesis of proteins. It is the only proteinogenic amino acid that contains a secondary amine that is part of its distinctive cyclic pyrrolidine ring structure (Figure 1). It is a non-polar aliphatic amino acid which is derived from L-glutamic acid **1.2** through a bifunctional enzyme, pyrroline-5-carboxylate synthase (P5C5S). This enzyme performs two consecutive processes: phosphorylation of L-glutamic acid to provide the intermediate substrate pyrroline-5-carboxylate (P5C) **1.3** through the action of glutamate kinase (GK), and reduction of the anhydride to its glutamyl- γ -semialdehyde **1.4** through γ -glutamyl phosphate (Pi) reductase (GPR). Spontaneous cyclization to form P5C **1.5** and reduction by pyrroline-5-carboxylate reductase (P5C5R) gives L-proline **1.6** (Scheme 1).^{1,2}

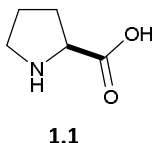
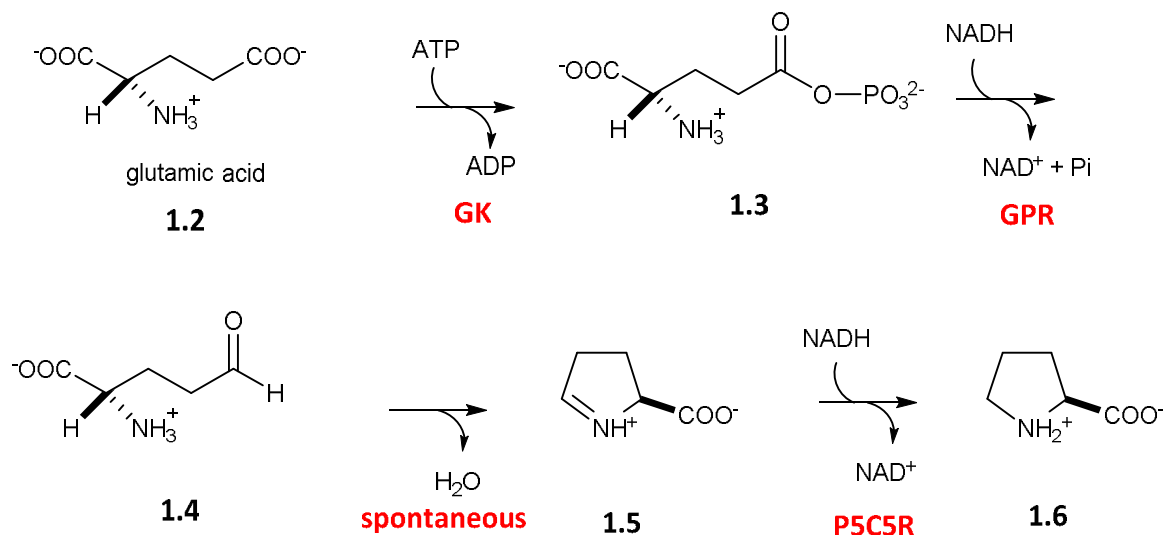


Figure 1. Chemical structure of L-Proline (Pro).

As a component of proteins and peptides, proline plays an important role in a variety of physiological activities. It is also known for its unique activity as an organocatalyst.³ There is great focus in understanding the geometric constraints that proline imposes on the conformations of folded and unfolded proteins. For example, proline is found in collagen, the most abundant fibrous protein in animals.⁴ A third of the protein content in humans is made up of collagen, which is the main component found in connective tissue in the body, such as the extracellular matrix, and fibrous tissues such as skin, tendons, and ligaments. There are twenty-eight types of collagen that are grouped based on the different structural motifs they form.⁴



Scheme 1. Biosynthesis of proline from glutamic acid.²

Collagen has a unique structure composed of a left-handed triple helix.^{4,5} Three polypeptide strands of polyproline II (PPII) type helices are held together through hydrogen bonds mainly between N- $\text{H}_{(\text{Gly})} \cdots \text{O}=\text{C}_{(\text{Xaa})}$ (Figure 2).⁴ This structural motif requires every third amino acid in each individual strand to be glycine (Gly). Collagen motifs contain a repeating sequence of Xaa-Yaa-Gly, where Xaa and Yaa can be any amino acid; however, most X-ray crystallography studies on collagen-related peptides (CRPs) have shown that Xaa and Yaa are usually (2S)-L-proline (Pro, 28%) and (2S,4R)-4-hydroxyproline (Hyp, 38%), respectively (Figure 2).

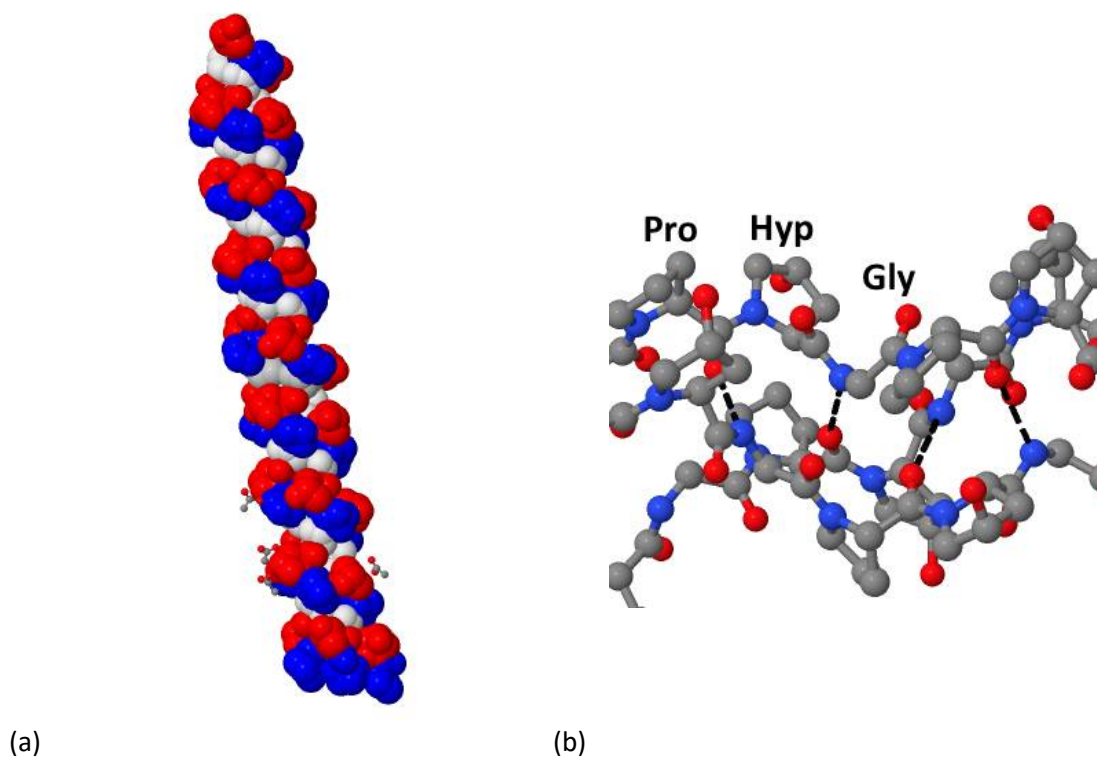


Figure 2. Collagen triple helix. (a) High-resolution crystal structure of the collagen triple helix. Amino acid labels: Pro (blue), Hyp (red), Gly (gray). (b) Ball-and-stick depiction of a segment of the collagen triple helix. Hydrogen bonds (black) between $\text{N-H}_{(\text{Gly})} \cdots \text{O}=\text{C}_{(\text{Xaa})}$ and $\text{C}^{\alpha}\text{-H}_{(\text{Gly})} \cdots \text{O}=\text{C}_{(\text{Yaa})}$. Atom Labels: carbon (gray), nitrogen (blue), oxygen (red). [Protein Data Bank (PDB) ID: 1CAG].

Proline derivatives can have different conformations, which in turn affect protein helix geometries. The pyrrolidine ring of Pro adopts one of two conformations dependent on the out-of-plane displacement of the γ carbon (C-4 gamma carbon atom, C_{γ}): $\text{C}_{\gamma}\text{-endo}$ **1.7** and $\text{C}_{\gamma}\text{-exo}$ **1.8** pucker conformations (Figure 3a). Proline has a slight preference for the $\text{C}_{\gamma}\text{-endo}$ pucker in *N*-acetylproline methyl ester;^{4,6} however, 4-substituted derivatives of Pro can prefer to adopt different C_{γ} puckers depending on the electronic character of the C_{γ} substituent. For example, the presence of a 4*R* electron-withdrawing group (EWG) in **1.9** exerts a gauche effect, where the EWG points towards the nitrogen atom stabilizing the $\text{C}_{\gamma}\text{-exo}$ **1.11** ring pucker (Figure 3b, c).^{4,7}

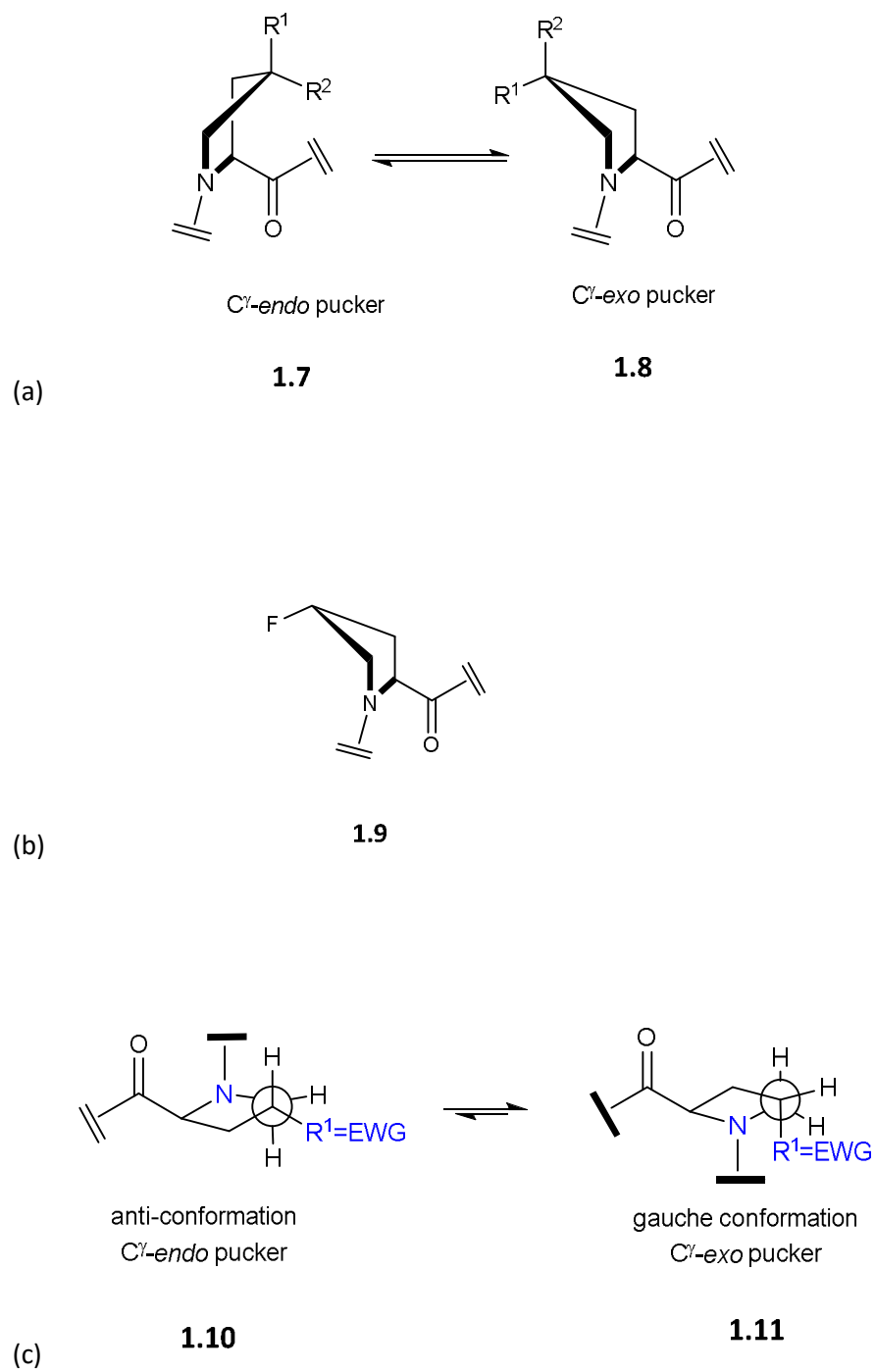


Figure 3. (a) *C γ -endo* and *C γ -exo* pucker conformations. (b) *C γ -exo* pucker conformation in the presence of an electron-withdrawing group in the 4*R* position as in (2*S*, 4*R*)-4-fluoroproline (flp). (c) The *C γ -exo* pucker in a gauche conformation is preferred due to stereoelectronic effects when $R^1 = \text{EWG}$.

In addition to substituent effects that influence the C γ ring pucker, another effect to consider with proline derivatives is the $n \rightarrow \pi^*$ interaction between amide carbonyl groups. In the $n \rightarrow \pi^*$ interaction, the carbonyl oxygen of the amide bond donates its lone pair to the antibonding orbital of the carbonyl of the adjacent peptide bond. The $n \rightarrow \pi^*$ interaction can only occur in the *trans*-peptide isomer, and has been reported to influence the $K_{trans/cis}$ ratios of the amide *N*-terminal to Pro derivatives. The C γ ring pucker may influence the $K_{trans/cis}$ ratio. A higher $K_{trans/cis}$ value is observed in the C γ -*exo* pucker **1.12** than the C γ -*endo* ring pucker (Figure 4).⁶⁻⁸ The C γ -*exo* pucker enhances the $n \rightarrow \pi^*$ overlap of the oxygen in the prolyl amide bond and the proline α -carbonyl **1.14**, which in turn provides greater $n \rightarrow \pi^*$ hyperconjugative delocalization of electrons.

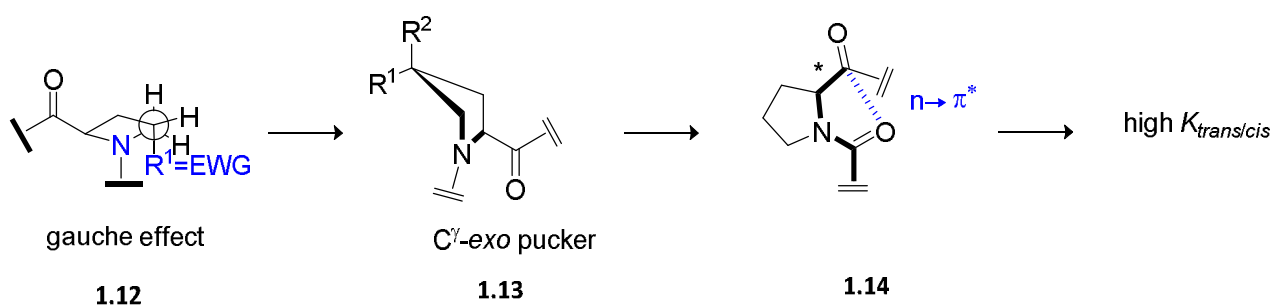


Figure 4. The presence of an electron-withdrawing group that exerts a gauche effect may consequently enhance the C γ -*exo* ring pucker and facilitate $n \rightarrow \pi^*$ stabilization leading to a high $K_{trans/cis}$ ratio.

Protein secondary structures are defined by the amino acid sequence that interacts intramolecularly through hydrogen bonds.⁹ α -Helices and β -sheets are the two most common secondary structures (Figure 5). Proline-rich polypeptide strands, however, may adopt two stable secondary structures: the polyproline type I helix (PPI) and the polyproline type II helix (PPII).⁵

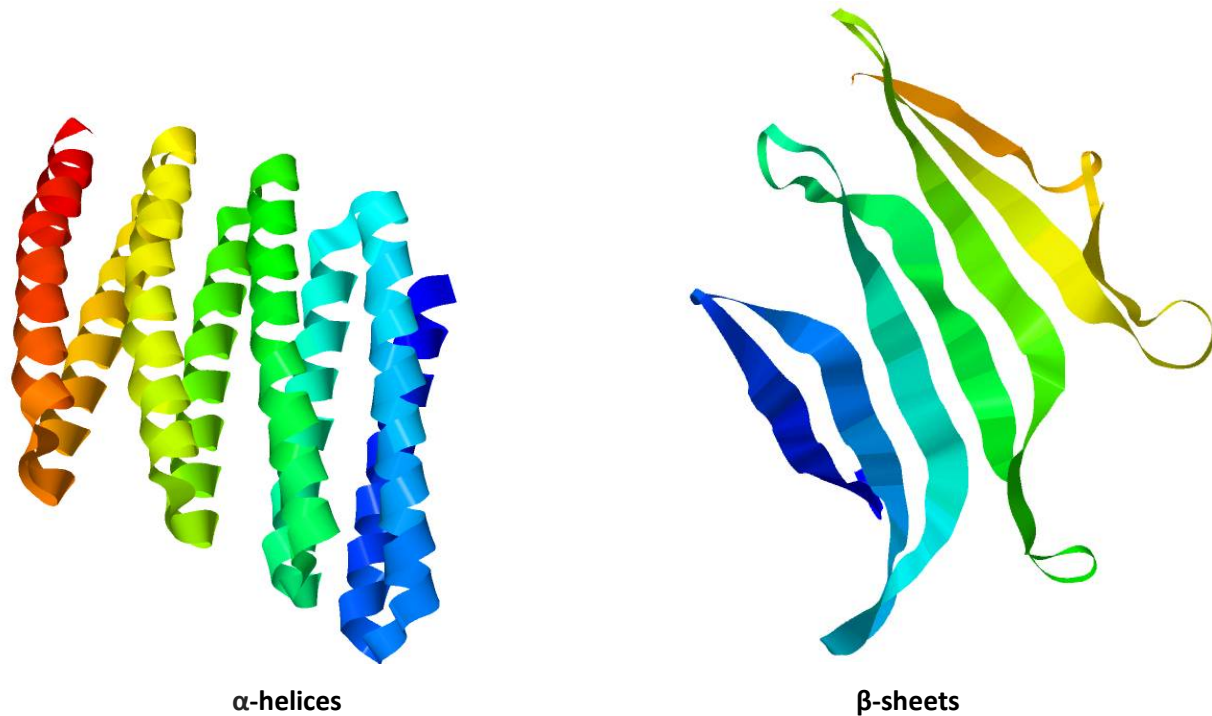


Figure 5. Secondary structures: α -helices and β -sheets. [PDB ID: α -helices – 5CWM, β -sheets – 5R80].

As opposed to α -helices and β -sheets, PPI and PPII helices do not employ intramolecular hydrogen bonds to stabilize their secondary structures; instead, geometric constraints lead to distinct orientations of the amide nitrogen and oxygen atoms. PPI has a right-handed helical structure comprised of all *cis*-peptide bonds and ideal ϕ , ψ , and ω backbone dihedral angles of -75° , $+160^\circ$, and 0° , respectively. On the other hand, PPII helices have a left-handed helical structure comprised of all *trans*-peptide bonds and ideal ϕ , ψ , and ω backbone dihedral angles of -75° , $+145^\circ$, and 180° , respectively. The PPI helix is compact and associated with a helical pitch of 5.6 \AA/turn and $3.3 \text{ residues/turn}$, whereas the PPII helix has a helical pitch of 9.3 \AA/turn and $3.0 \text{ residues/turn}$, thus making it more extended than the PPI structure (Figure 6).⁵

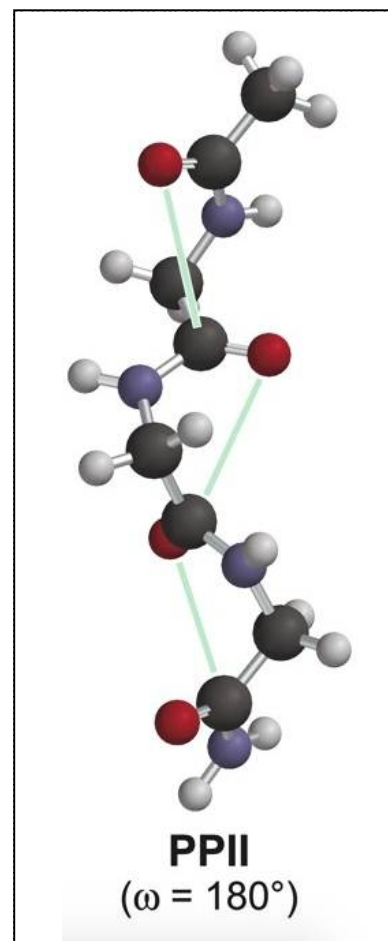
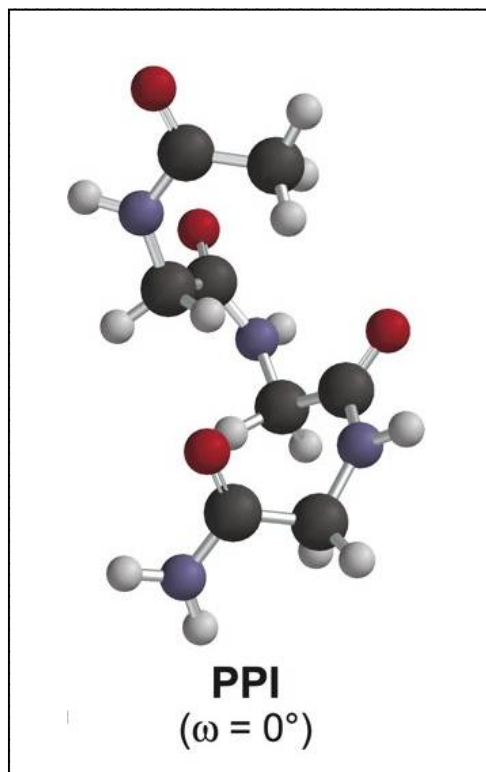


Figure 6. Polyproline type I (PPI) right-handed helix comprised of all *cis*-peptide bonds. Polyproline type II (PPII) left-handed helix comprised of all *trans*-peptide bonds in which the green lines depict the favorable presence of the $n \rightarrow \pi^*$ stabilization.⁵

PPII is found in various types of proteins, and plays an important role in multiple biological processes, such as transcription, translation, signal transduction, and immune response.⁵ PPII has great importance in protein structure and function, in part due to its high conformational stability. PPII helicity dominates in aqueous solution, whereas PPI is favored in organic solvents.⁵ Consequently, PPII is very commonly found in folded and unfolded proteins, whereas PPI helices are rarely associated with biological phenomena.^{5, 10}

cis- and *trans*-4,5-Methano-L-proline

Previously, our group synthesized *cis*- and *trans*-4,5-L-methanoprolines **1.15** and **1.16**.¹¹ Based on X-ray crystallographic evidence, the structures of *cis*- and *trans*-4,5-L-methanoprolines indicated a more planar ring conformation compared to proline (Figure 7).¹¹ The presence of the cyclopropane ring may affect the properties of prolyl amides in several ways. For example, the added ring may influence the level of hybridization of the nitrogen atom (planar vs. pyramidal), which in turn could affect the *cis/trans* amide isomer ratio. With such distinctive characteristics in mind, proline residues of various drugs were replaced with *cis*- and *trans*-4,5-L-methanoprolines.

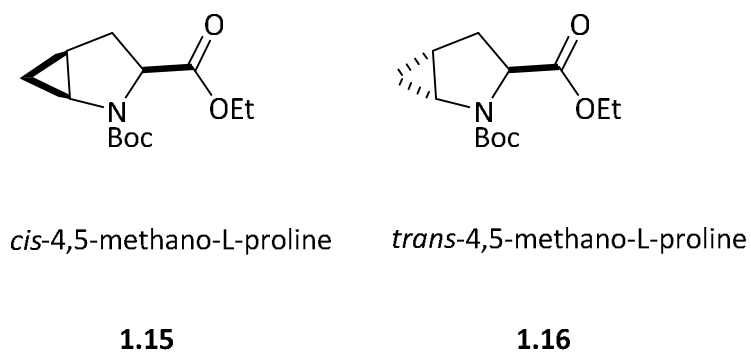


Figure 7. *cis*- and *trans*-4,5-methano-L-proline.

For instance, the antidiabetic drug Onglyza (saxagliptin) incorporates a 4,5-methano-L-proline nitrile as part of its structure.¹² Type II diabetes is a widespread metabolic condition that is characterized by high blood sugar (hyperglycemia) due to either lack of insulin or insulin resistance.¹³ Glucagon-like peptide 1 (GLP-1) is a hormone secreted in the body that is required for glucose-stimulated insulin secretion. However, dipeptidyl-peptidase IV (DPP-IV), an enzyme with a wide variety of substrates, is responsible for the degradation of GLP-1, which consequently prevents the secretion of insulin leading to hyperglycemia (Figure 8).¹³

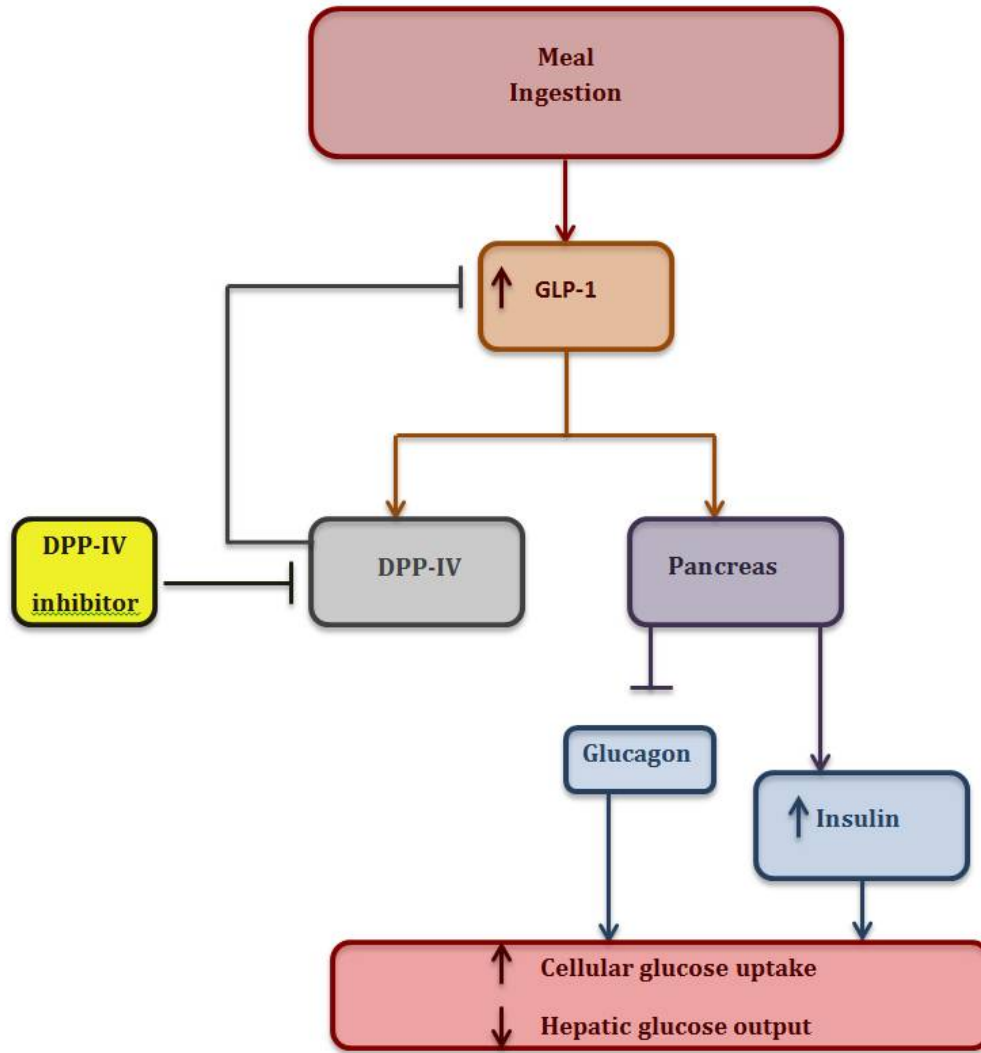


Figure 8. Inhibitory pathway of DPP-IV on GLP-1.¹³

Several DPP-IV inhibitors have been reported to inhibit GLP-1 cleavage activity.^{12,13} The early DPP-IV inhibitors consisted of proline-based dipeptide derivatives bearing various functional groups such as boronic acids **1.17** and diphenyl phosphonates **1.18**, (Figure 9).¹³ However, these compounds had limited efficacy because they either irreversibly inhibited the DPP-IV enzyme or were slowly released from the enzyme. Usually, irreversible enzyme inhibitors are not suitable because they can remain attached to the target protein and may cause adverse effects. Consequently, reversible inhibitors comprised of the same proline dipeptide core containing nitrile substituents were developed, (Figure 9 – **1.19**).¹³ Although this generation of compounds proved to be potent inhibitors, they were nonetheless chemically unstable due to the intramolecular cyclization caused by the nucleophilic attack of the primary amino group in the adamantyl side chain onto the nitrile group.¹³ Therefore, other DPP-IV inhibitors were developed with better chemical stability by the incorporation of more hindered alkylamines or by the omission of the nitrile moiety (Figure 9 – **1.20-1.23**), to prevent intramolecular cyclization.¹³

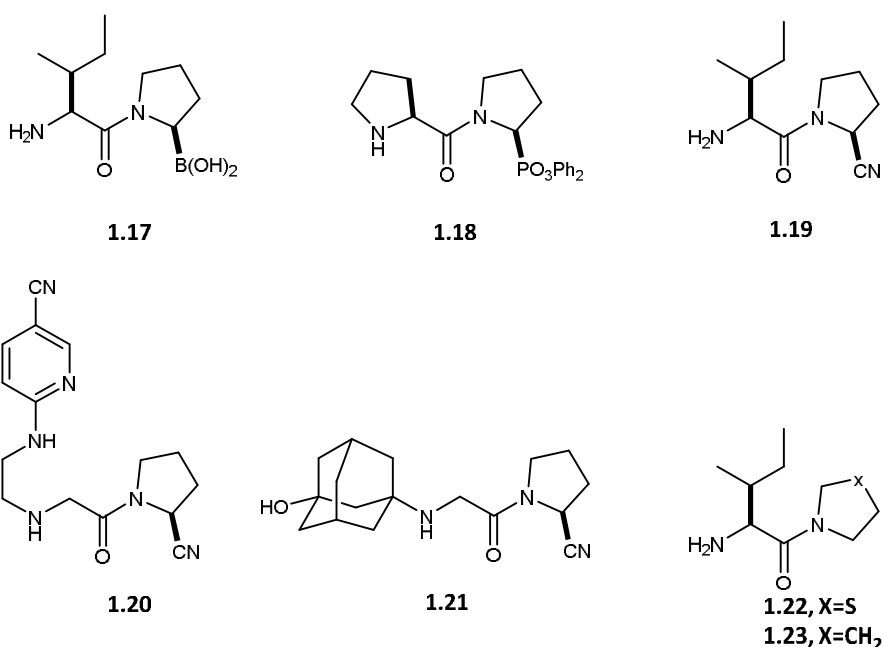


Figure 9. Early generations of proline-based dipeptide peptidase IV inhibitors.¹³

Magnin and coworkers, sought to find an alternative motif to improve DPP-IV inhibitor potency by altering the core conformation of the inhibitor rather than modifying the functional groups present in the drug.¹² Inspired by the reported flattening of the proline ring when installing a 4,5-methano moiety as described by the Hanessian group,¹¹ Magnin *et al.*, incorporated the *cis*-4,5-methanoproline in the dipeptide system, which led subsequently to the discovery of a stable and potent DPP-IV inhibitor, now marketed as Onglyza.¹² In the process, the scientists at Bristol-Myers Squibb investigated other methanoproline analogs **1.24-1.31**, which were found to be less effective as Onglyza. For example, the other seven stereoisomers of the methanoproline analogs were synthesized and possessed lower efficacy as DPP-IV inhibitors (Figure 10).¹²

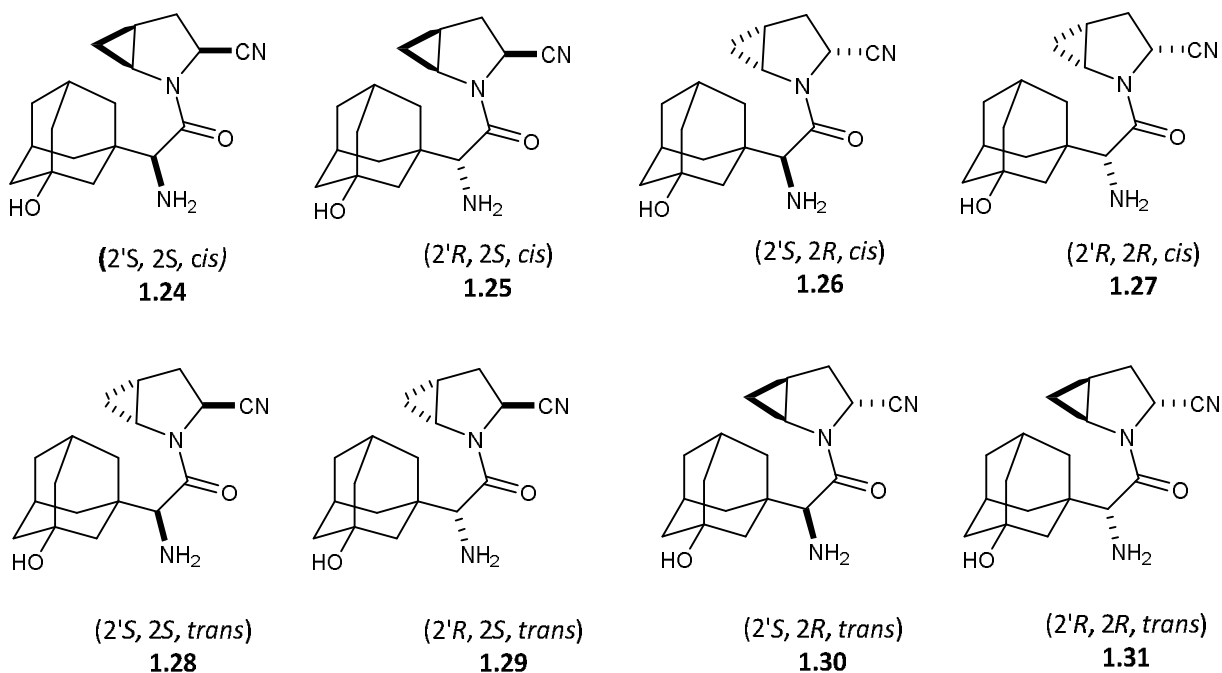


Figure 10. The eight stereoisomers of Onglyza.¹²

Conformational Comparisons Between Proline and 4,5-Methano-L-proline Oligomers

Crystallization of proline oligomers can be difficult.¹⁴ Although crystal structures of proline dimers, trimers, and tetramers were previously obtained,¹⁵ none exhibited the PPII secondary structure. Wennemers and coworkers succeeded in obtaining the crystal structure of a hexameric polyproline **1.32** displaying the PPII helical motif (Figure 11).¹⁴ The crystal structure showed that there was a C_3 -symmetry axis along the helical axis, which is in agreement with the PPII helix geometry. However, a slight distortion of the backbone atoms was observed because of differences in the dihedral angles (ϕ and ψ) and ring puckering of the six proline residues in the hexamer (Table 1).¹⁴

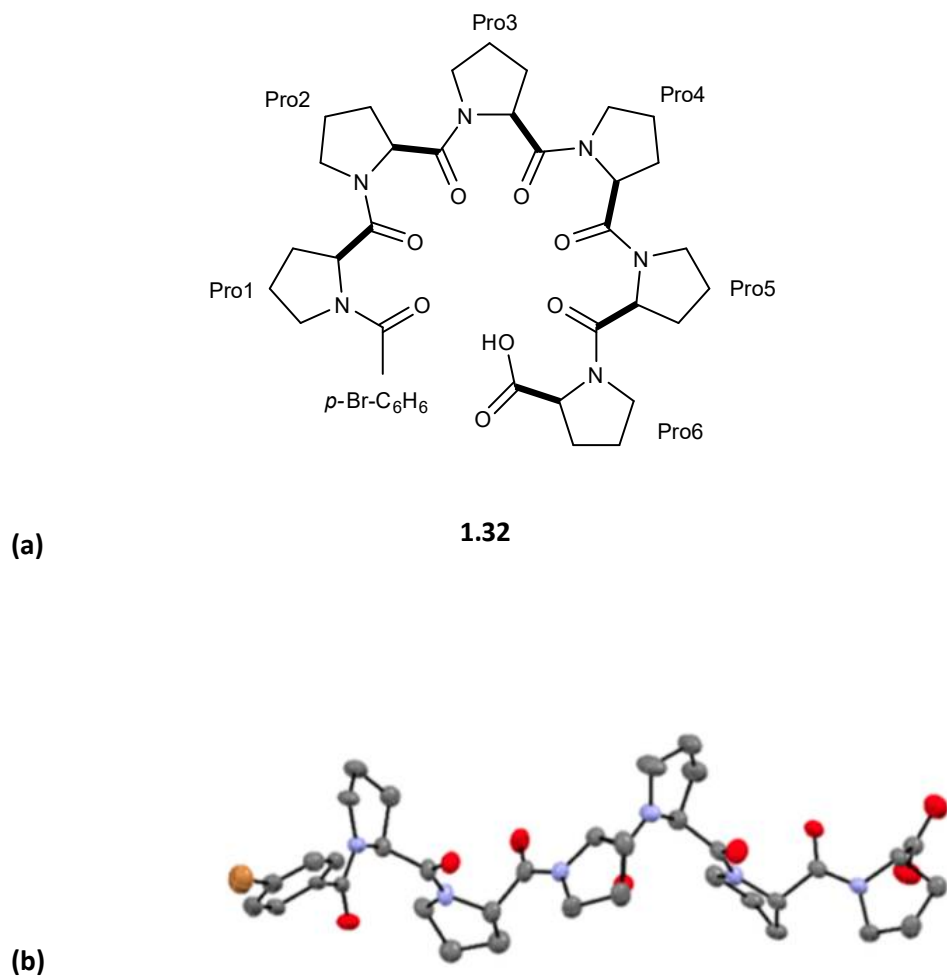


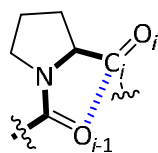
Figure 11. (a) Proline hexamer $p\text{-Br-C}_6\text{H}_4\text{-Pro}_6\text{-COOH}$. (b) Crystal structure of the polyproline hexamer.¹⁴

Statistical database analysis of proline residues in crystallized protein structures shows a correlation between the proline residue dihedral angles and the resulting ring pucker. The closer the dihedral angles, ϕ and ψ , are to -65° and $+140^\circ$, the more likely a *C γ -exo* pucker is formed.^{14, 16} This trend was observed in the crystalline hexameric proline oligomer: the initial sequence residues Pro1 and Pro2 had a *C γ -exo* pucker, residues Pro3-Pro5 showed twisted *C γ -endo* pucker, and Pro6 had a twisted *C γ -exo* ring pucker (Table 1).¹⁴

Table 1. Ring puckering and ϕ and ψ of the proline hexamer.¹⁴

residue	ϕ	ψ	ring pucker
Pro1	-67.1°	$+143.6^\circ$	<i>Cγ-exo</i>
Pro2	-65.7°	$+138.0^\circ$	<i>Cγ-exo</i>
Pro3	-73.1°	$+163.9^\circ$	twisted <i>Cβ-exo- Cγ-endo</i>
Pro4	-72.8°	$+151.0^\circ$	twisted <i>Cβ-exo- Cγ-endo</i>
Pro5	-72.5°	$+165.2^\circ$	twisted <i>Cβ-exo- Cγ-endo</i>
Pro6	-69.0°	$+150.3^\circ$	twisted <i>Cβ-endo- Cγ-exo</i>

Although previous findings have suggested that the PPII helix can only form in the presence of coordinating water molecules, Wennemers and coworkers showed that the hydration was not required for its stabilization.^{10, 14} Analysis of the distances, trajectory angles, and pyramidalization of C_i , as well as the distances between the α -carbonyl carbons and prolyl carbonyl oxygens revealed the existence of $n \rightarrow \pi^*$ stabilization as depicted in **1.33** (Figure 12).¹⁴



$n \rightarrow \pi^*$ interaction

1.33

Figure 12. Depiction of $n \rightarrow \pi^*$ interaction in a PPII helix.¹⁴

Hanessian and coworkers reported the first examples of polyproline derivatives based on repeating units of *cis*-4,5-methano-L-prolines, the tetramer of which adopted a PPII conformation.¹⁷ Monomers of *cis*- and *trans*-4,5-methano-L-prolines were coupled to form dimers, tetramers, and hexamers that were analyzed by X-ray diffraction (XRD) and circular dichroism (CD) spectroscopy. The CD curve for PPII-type helices is characterized by a strong negative maximum at 206 nm and a positive maximum at 225 nm.¹⁷ Results from the work of Dr. Gilles Berger in the Hanessian group shows the CD spectra of the *cis*-4,5-methano-L-proline oligomers to have similar characteristics to that of a PPII helix whereas the *trans*-4,5-methano-L-proline counterparts are disordered under the same conditions.¹⁷ The crystal structure of the *cis/cis*-4,5-methano-L-proline (*cis-cis*) dimer shows a *trans*-peptide bond with a ψ angle around 165° resulting in a distance less than the sum of the Van der Waals radii between the adjacent carbonyl groups, which indicates the existence of the $n \rightarrow \pi^*$ stabilization.¹⁷ The distances between the amide carbonyl oxygen and the adjacent carbonyl group of the *trans/trans*-4,5-methano-L-proline dimer (*trans-trans*) and the *trans/cis*-4,5-methano-L-proline dimer (*trans-cis*) are also less than the sum of the Van der Waals radii, nonetheless longer than in the *cis-cis*, implying weaker $n \rightarrow \pi^*$ stabilization.¹⁷ Moreover, the trajectory angles of the carbonyls in the *trans-trans* and the *trans-cis* analogs are between 85° and 98° , which do not lie within the ideal Bürgi-Dunitz angle of 107° required for the spatial proximity to the C_i carbonyl group.¹⁷

Furthermore, DFT (ω B97x-D/def2-TZVP) and NBO analysis conducted by Dr. Berger revealed that the *trans-trans* and the *trans-cis* have a significantly lower stabilization in the $n \rightarrow \pi^*$ delocalization due to non-complimentary overlap between the acceptor antibonding orbital of the C_i amide carbonyl, and the donor amide carbonyl respectively.¹⁷ Because of higher energetic contribution of the $n \rightarrow \pi^*$ interaction, the *cis/cis*-4,5-methanoproline dimer possesses a stronger overall stabilization to adopt the *trans*-amide conformation, which in turn induces the formation of the PPII helical conformation.¹⁷

As previously reported by Raines, one factor that largely stabilizes the PPII helical conformation is attributed to $n \rightarrow \pi^*$ stabilization.¹⁸ Wennemers and Raines both reported that *N*-acetyl proline methyl ester favors the *trans*-amide conformer rather than the *cis*-amide conformer.^{18, 19, 20} Among various factors that influence the *trans* : *cis* equilibrium of Xaa-Pro bonds, the $n \rightarrow \pi^*$ interaction between the adjacent carbonyl groups is significant. Wennemers and coworkers conducted various experiments to determine the *trans* : *cis* equilibrium of Xaa-Pro bonds in polar and apolar environments. Although the *trans*-amide conformation dominates, the ratios vary in solvents of different polarities.²⁰ These variations are due to environmental changes that may affect the amide conformation and in turn the $n \rightarrow \pi^*$ stabilization. Theoretically, a lower *trans* : *cis* ratio should be observed in polar solvents due to interactions between the carbonyls and the solvent. In apolar solvents, less interactions of the carbonyls with solvent may account for a higher *trans* : *cis* ratio.

Diketopiperazine Formation

Peptide and protein chains with free amines at the *N*-termini can undergo acid- or base-catalyzed intramolecular aminolysis to form diketopiperazines.²¹ The degradation involves a nucleophilic attack of the *N*-terminal free amine onto the amide carbonyl of the *C*-terminal amino acid residue. The cyclization reaction is accelerated by the presence of certain amino acids such as proline, glycine, D-amino acids, and *N*-methylamino acids.²¹ Most amino acids adopt *trans*-amide conformations in proteins, however, as previously mentioned, proline may adopt either the *cis*- or *trans*-amide conformation. This property facilitates proline's rapid diketopiperazine formation because cyclization can only occur in the *cis*-amide conformation.²²

The cyclization reaction to a DKP follows pseudo-first order kinetics and is affected by various factors such as temperature, pH, concentration, and the nature of the buffer.²³ At a pH below 3.0, the amine exists in its protonated form, which is not favorable for cyclization. In basic media (pH 9.0-10), the cyclization is first order in hydroxide ion making it a specific base catalysis.²³ The rate was shown to be directly proportional to increasing pH between 4.0-6.0 and seemed to plateau between pH 6.0-8.0, where the cyclization occurs through a neutral-catalyzed pathway. Nevertheless, further hydrolysis at either carbonyl group **1.36** is possible leading to the formation of two different dipeptides **1.37** and **1.38** (Figure 13).²³

As anticipated by the Arrhenius equation, the rate of cyclization increased with increasing temperature at all pH values.²⁴ Further studies were conducted to analyze the effects of different amino acids positioned on the *N*-terminal side of the proline residue. The rate of cyclization was predicted to be affected by amine pK_a and conformation; however, these factors were not found to influence the rate of diketopiperazine formation.²³ Since the nucleophilic attack of the amine nitrogen onto the ester can only occur in the *cis*-amide conformation **1.35**, the rate of cyclization should depend on the energy barrier for

trans to *cis* isomerization. The smaller the energy barrier for *trans* to *cis* isomerization, the faster the rate of cyclization.²³

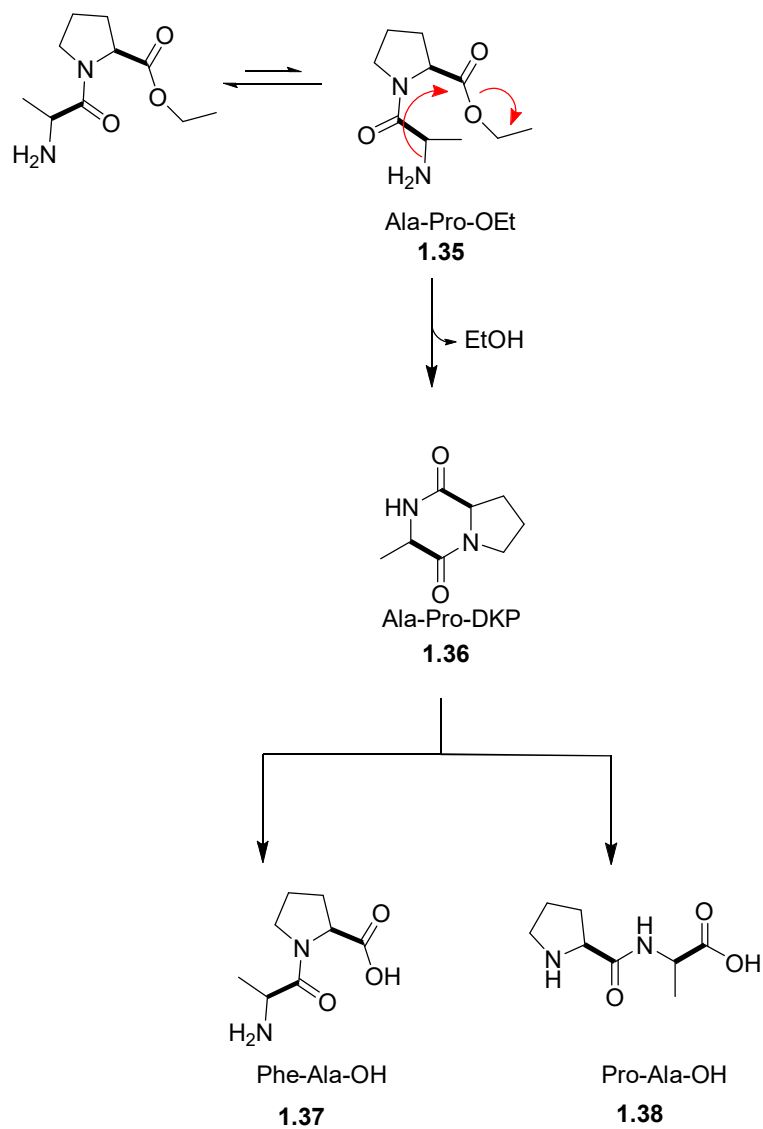
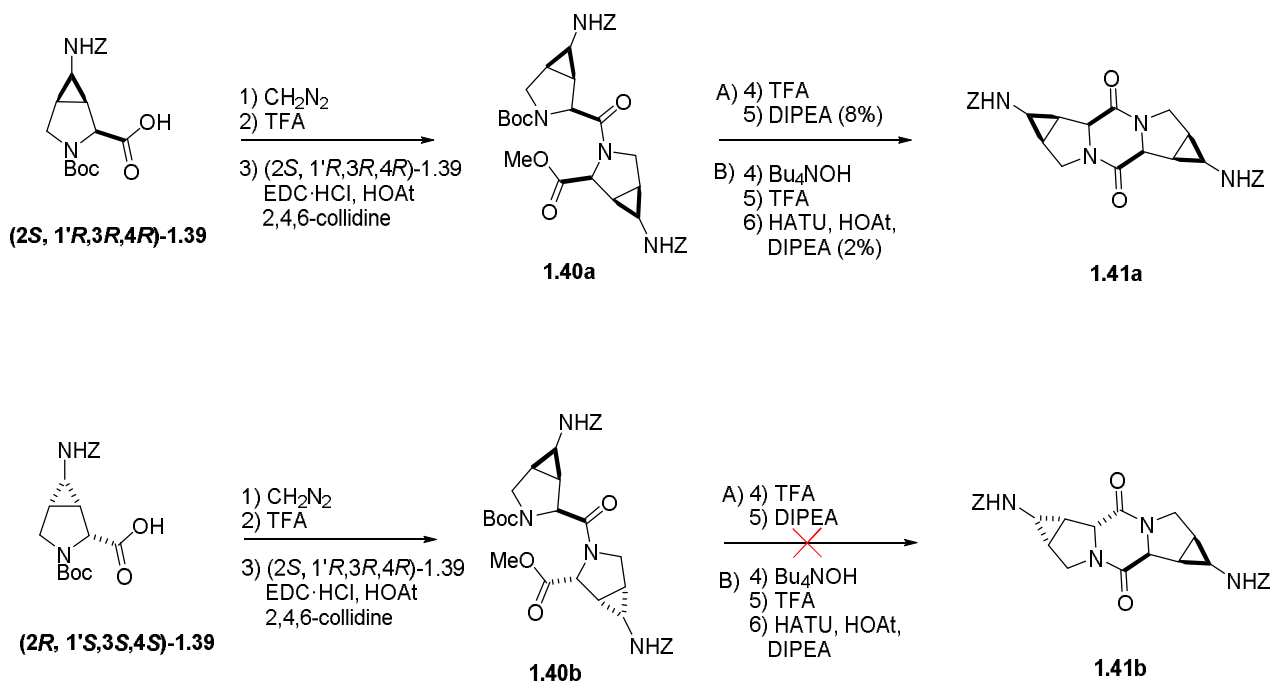


Figure 13. The diketopiperazine formation of Ala-Pro-COOEt into Ala-Pro-DKP and ethanol. Hydrolysis of Ala-Pro-DKP may form either Ala-Pro-OH or Pro-Ala-OH at pH <3.0 and > 8.0.²⁴

A diketopiperazine formation study on 3,4-(aminomethano)proline (Amp) has previously been conducted.²⁵ Diketopiperazines **1.41a** and **1.41b** were synthesized from (2*S*,1'*R*,3*R*,4*R*)-**1.39** and (2*R*,1'*S*,3*S*,4*S*)-**1.39** (Scheme 2).²⁵ The rate of diketopiperazine formation varied with condition. After Boc group removal, methyl ester **1.40a** cyclized under basic conditions using DIPEA to give **1.41a** in 8% yield over five steps.²⁵ Attempts to form diketopiperazine **1.41a** after Boc deprotection and hydrolysis of methyl ester **1.40a** using HATU, HOAt, and DIPEA resulted in 2% yield over six steps.²⁵ Diastereomer **1.40b** did not cyclize to the corresponding DKP after deprotection of the Boc group and treatment under basic conditions.²⁵



Scheme 2. Diketopiperazine synthetic route of 3,4-(aminomethano)proline.²⁵ Difficulty of diketopiperazine cyclization of the *cis-cis* dimer.

In this thesis, the structural characteristics of *cis*- and *trans*-4,5-methano-N-acetyl L-proline methyl esters are studied with regards to the *trans* : *cis* equilibrium of the amide geometry in different solvents. The propensities for cyclization of *cis-cis*, *trans-trans*, and *trans-cis* dimer ethyl esters to DKPs will also be presented.

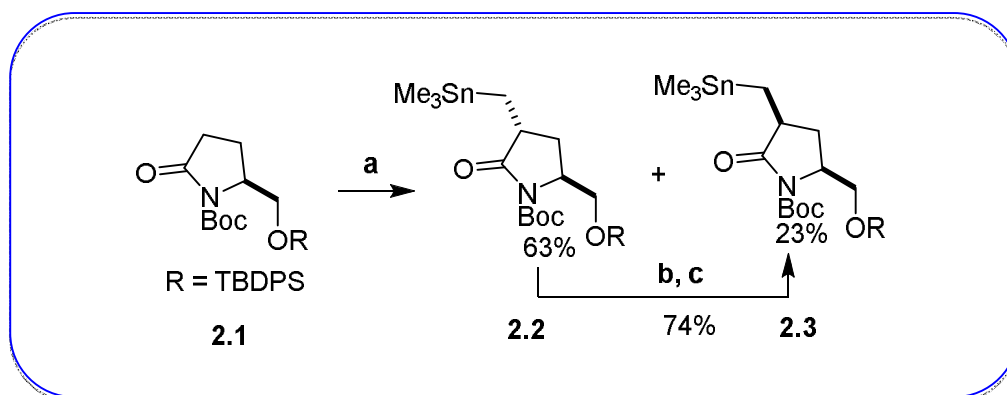
Results and Discussion

Synthesis of *cis*- and *trans*-4,5-methano-L-proline

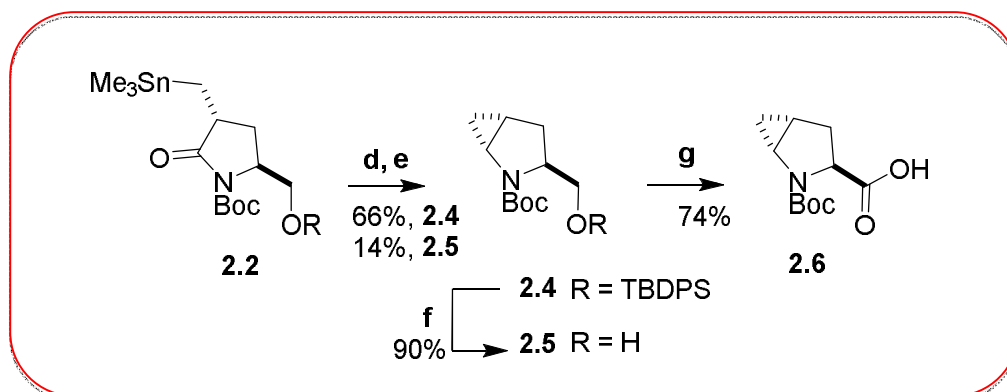
The synthesis of various proline derivatives has great importance in the peptidomimetic field of research.⁴ The synthesis of 4,5-methanoprolines was initially reported by Hanessian *et al.*¹¹ The first synthetic protocol described a stereocontrolled syntheses of 4,5-methano-L-prolines through an intramolecular carbocyclization reaction involving stannane-based cyclopropanation (Scheme 3a).¹¹ This novel reaction afforded a 3:1 mixture of diastereoisomers which could be separated by chromatography to give **2.2** and **2.3** starting with the readily available lactam **2.1**. The *anti*-isomer **2.2** could be converted to the *syn*-isomer **2.3** through enolate formation and subsequent protonation with the hindered acid 2,6-di-*tert*-butylphenol.

The *anti*-isomer organostannane lactam **2.2** was reduced to the hemiaminal and treated with trifluoroacetic acid to afford exclusively the *trans*-4,5-methano-L-proline analog **2.6** in 66% yield over two steps (Scheme 3b). Employing amination derivative **2.7** (Scheme 3c), the *cis*-4,5-methanoprolines **2.8** was synthesized.¹¹

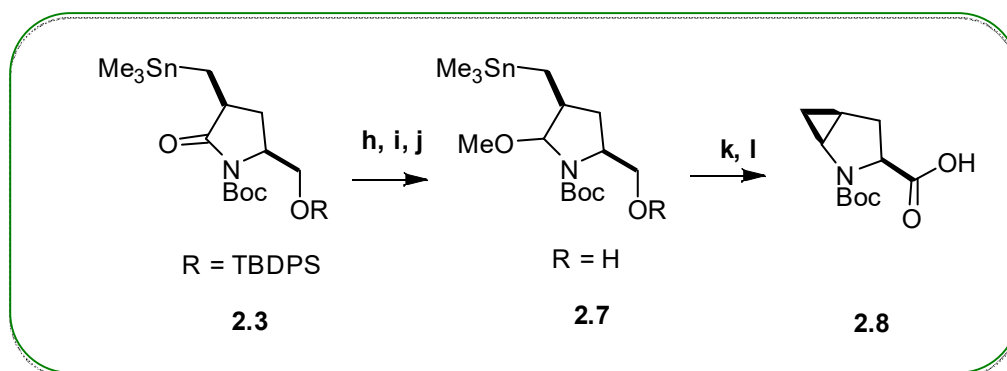
(a)



(b)



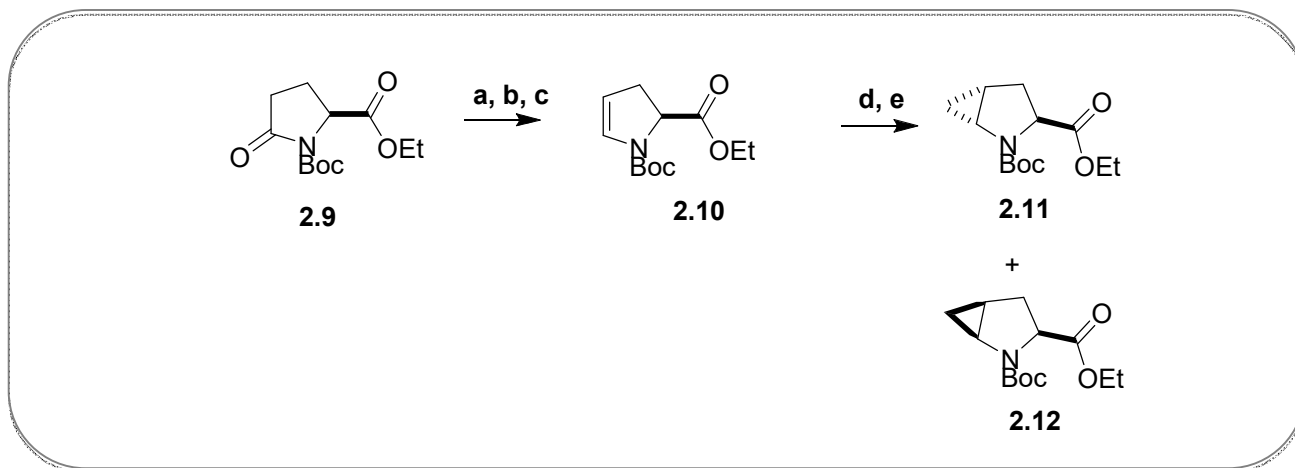
(c)



Scheme 3. (a) LiHMDS, THF, -78 °C, then Me₃SnCH₂I, -30 °C, 63% (**2.2**) and 23% (**2.3**). (b) LiHMDS, THF. (c) 2,6-di-*tert*-butylphenol, -78 °C, 74%. (d) LiEt₃BH, THF. (e) TFA, CH₂Cl₂, 66% (**2.4**) and 14% (**2.5**). (f) Bu₄NF, THF, 90%. (g) RuCl₃, NaIO₄, CCl₄/CH₃CN/H₂O, 75%. (h) LiEt₃BH, THF. (i) MeOH, CSA. (j) Bu₄NF/AcOH, THF, 83%. (k) TFA, CH₂Cl₂, 79%. (l) RuCl₃, NaIO₄, CCl₄/CH₃CN/H₂O, 71%.

Although the initial synthetic procedure gave *cis*- and *trans*-4,5-methano-L-proline diastereoselectively, Hanessian *et al.* explored a second approach involving the Simmons-Smith-Furukawa (SSF) cyclopropanation reaction starting from the commercially available L-pyroglutamic acid **2.9** (Scheme 4).²⁶ Lactam **2.9** was converted to the ene-carbamate **2.10** upon treatment with lithium triethylborohydride, followed by the formation of the methoxy hemiaminal and elimination of methanol. Subsequently, during the SSF-cyclopropanation of dihydropyrrole **2.10**, the Boc group was removed and later reinstalled to give **2.11** and **2.12**, by an additional step. This procedure yielded successfully a 1:4

diastereomeric mixture of *cis*-4,5-methanoproline **2.12** and *trans*-4,5-methanoproline **2.11** that was separated by column chromatography.



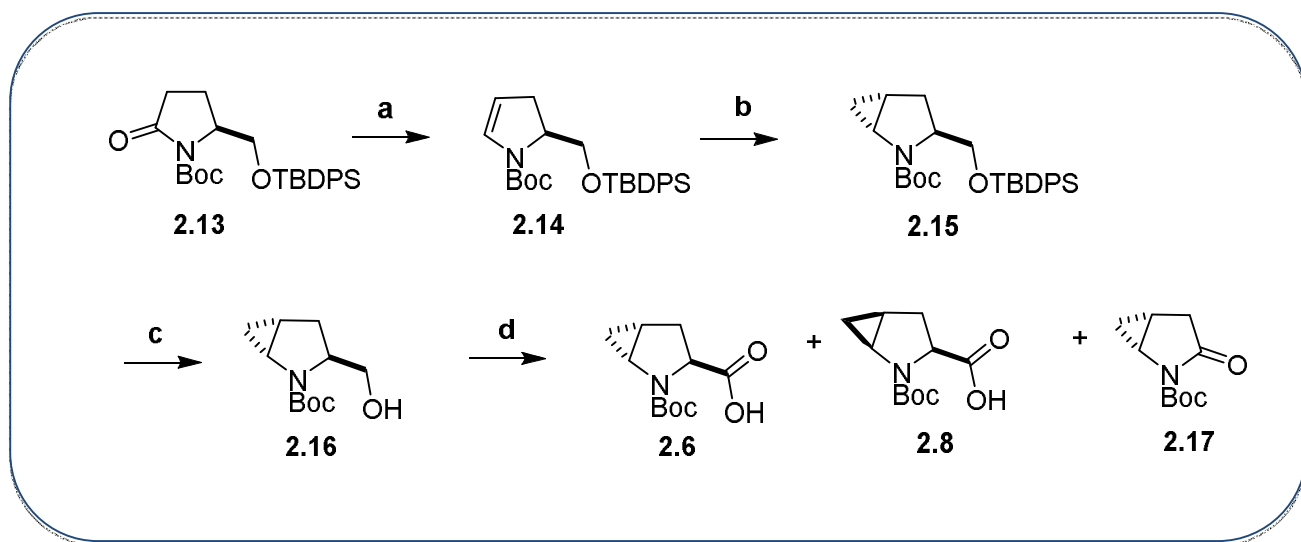
Scheme 4. (a) LiEt_3H , THF, 95%. (b) PPTS, MeOH. (c) NH_4Cl , 150 °C, 20-100 mmHg, 81%. (d) $\text{Et}_2\text{Zn}/\text{CH}_2\text{I}_2$, 65%. (e) Boc_2O , DMAP, Et_3N , CH_2Cl_2 , 75%.

More recently, Wang *et al.* described a new synthetic protocol with slight modifications to the procedure reported by Hanessian that resulted in enhanced stereoselectivity.²⁷ By lowering the temperature of the SSF-cyclopropanation from 0 °C to -23 °C and by using chloriodomethane instead of diiodomethane, the *trans* : *cis* ratio improved from 1:4 to ~ 1:11 without loss of the Boc group.

Following this, the potential factors leading to high *cis* selectivity showed the C- α ester functional group to play an important role by chelating the resultant ' IZnCH_2Cl ' moiety and directing cyclopropanation on the same-face as the ester, resulting in the *cis*-4,5-methano-L-proline **2.12**.²⁸ Further investigations were carried out in hopes of finding a suitable functional group that would yield the *trans*-4,5-methano-L-proline as the dominant isomer.

To promote the *trans*-facial selectivity, a bulky silyl ether was used to inhibit the chelation of the putative 'IZn₂Cl' species and occupy the spatial surroundings of the *syn*-face. Cyclopropanation of the alkene on the opposing face of the C- α functional group yielded the *trans*-4,5-methanoproline **2.6** with a *trans* : *cis* ratio of 25:1 (Scheme 5).²⁷

Wang and coworkers improved the synthetic procedure for the *cis*-4,5-methano-L-proline **2.12** with a greater *trans* : *cis* ratio of 1:11, and devised a new synthetic route for the synthesis of *trans*-4,5-methano-L-proline **2.6** with a *trans* : *cis* ratio of 25:1 by manipulating the chelating capacity of the C- α functional group.²⁷ These two procedures were used to synthesize the monomeric *cis*- and *trans*-4,5-methano-L-prolines **2.12** and **2.6**, respectively.



Scheme 5. (a) LiBHET₃, TFAA/DIPEA, DMAP, toluene, -78 °C to r.t., (b) Et₂Zn, ICHCl, toluene, -35 °C, (c) TBAF, THF, rt (d) RuCl₃, NaIO₄, CCl₄/ACN/H₂O, rt.

Electronic Effects on the *trans-cis* Isomerization Equilibrium

With the proline methanologues in hand, we attempted to analyze the influence of the methylene bridge on the *cis*- and *trans*-peptide bond isomerization. Initially, DFT calculations were performed and compared with similar experiments as those reported by Raines and Wennemers.^{18, 20} In the case of prolyl amide **2.18**, the efficiency of the $n \rightarrow \pi^*$ stabilization has been attributed to complement steric effects that favor the *trans*-isomer. Raines revealed that the electron delocalization between the adjacent carbonyl groups in proteins may depend on the capacity of the lone pair of the amide oxygen (n) to overlap the antibonding orbital of the adjacent carbonyl carbon (π^*).¹⁸ The *trans*-conformer should be favored relative to the *cis*-conformer due to the shorter proximity between the amide oxygen lone pair to the adjacent antibonding orbital of the ester carbonyl.

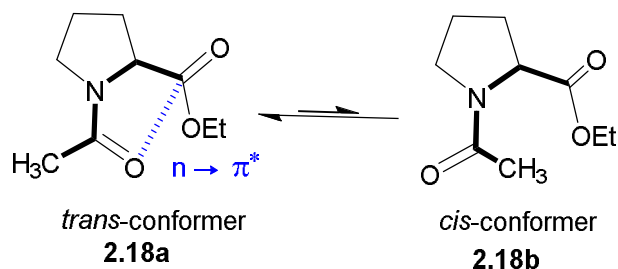


Figure 14. *Cis* : *trans* isomerization of the Ac-Pro-OEt amide bond.

Experimental studies were conducted to confirm these hypotheses. Raines¹⁸ and Wennemers²⁰ conducted similar studies describing *trans* : *cis* isomerization of *N*-acetyl proline methyl ester **2.19** (Ac-Pro-OMe) under various solvent conditions. ¹H NMR spectroscopy of Ac-Pro-OMe **2.19** and a tertiary amide Ac-Pro-NMe₂ **2.20** were recorded in relatively polar (D₂O, DMSO-d₆), and nonpolar (CDCl₃, dioxane-d₈)

solvents (Figure 15).²⁰ Although the *trans*-amide isomer predominated in all solvents, higher *cis*-isomer populations were observed in polar solvents compared to nonpolar solvents.²⁰ Besides sterics and $n \rightarrow \pi^*$ stabilization, a correlation between solvent polarity and *trans* : *cis* conformer equilibrium of Xaa-Pro bonds was revealed.²⁰

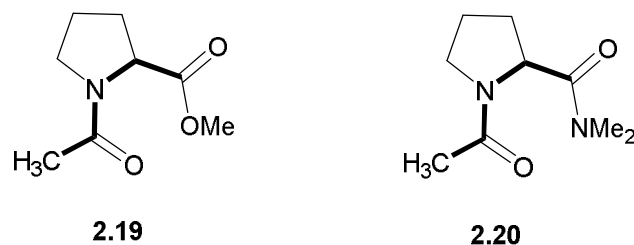
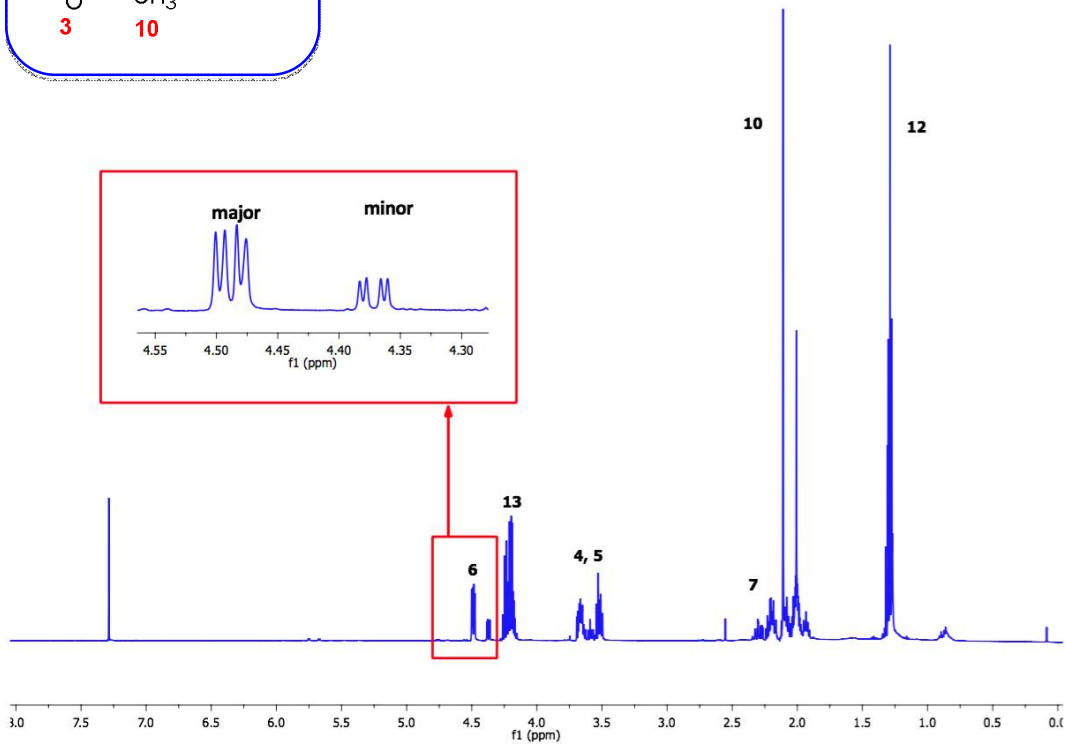
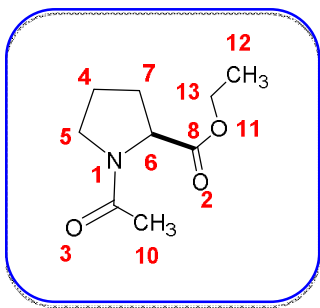


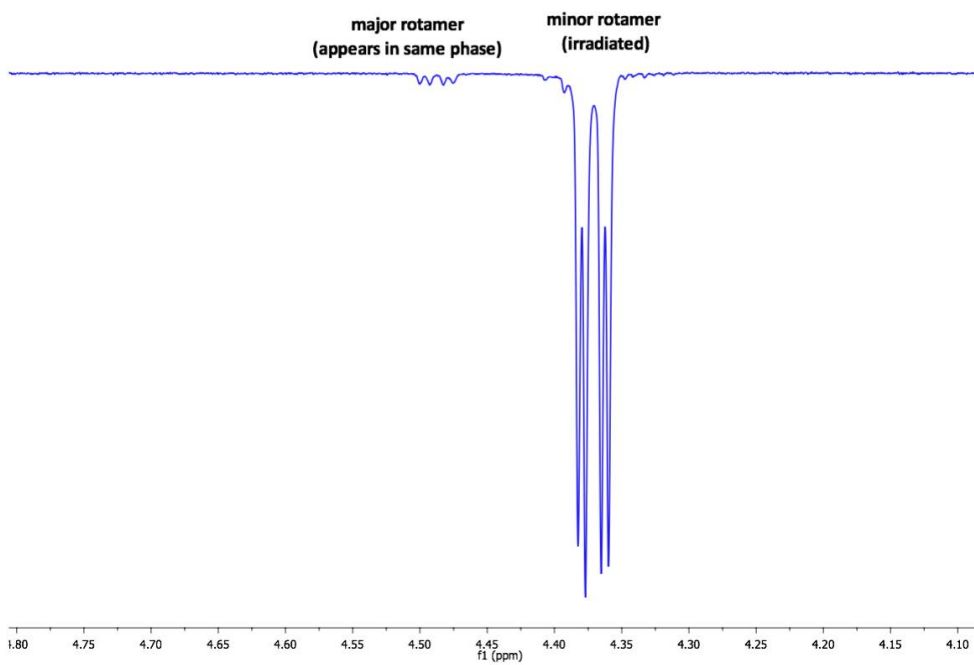
Figure 15. Ac-Pro-OMe and tertiary amide Ac-Pro-NMe₂.

Different $K_{trans/cis}$ ratios are expected between proline, and *trans*- and *cis*-4,5-methano-L-prolines due to their spatial and conformational differences. NBO and DFT analyses conducted by Dr. Gilles Berger in the Hanessian group revealed the free energy gaps for the *trans* : *cis* amide isomerization to be slightly higher for the 4,5-methanoproline congeners than for proline.¹⁷ NBO studies also showed the cyclopropane carbon atoms (C₆) fused to the pyrrolidine ring to have higher sp^2 character which renders the rings nearly co-planar and flattens the proline ring.¹⁷ Proline exhibits strong sp^3 -type character for the same bonding orbitals. Both *cis*- and *trans*-4,5-methano-L-prolines, **2.12** and **2.11**, respectively, were found to have shorter C-N bonds than proline, consistent with greater sp^2 -type character of C₆.¹⁷

We prepared *cis*- and *trans*-ethyl *N*-acetylated-4,5-methano-L-prolinates (*cis*- and *trans*-Ac-MPro-OEt, **2.21** and **2.22**, respectively) using previously published protocols. Ethyl (*N*-acetyl)-prolinate **2.18** was used as control. The ¹H NMR spectra of all three proline analogs **2.18**, **2.21** and **2.22** have two different sets of signals, corresponding to the major *trans*- and minor *cis*-amide isomers (Figure 16). In their 1D NOE spectra, the signals of the two isomers exhibit the same phase due to exchange.



(a)



(b)

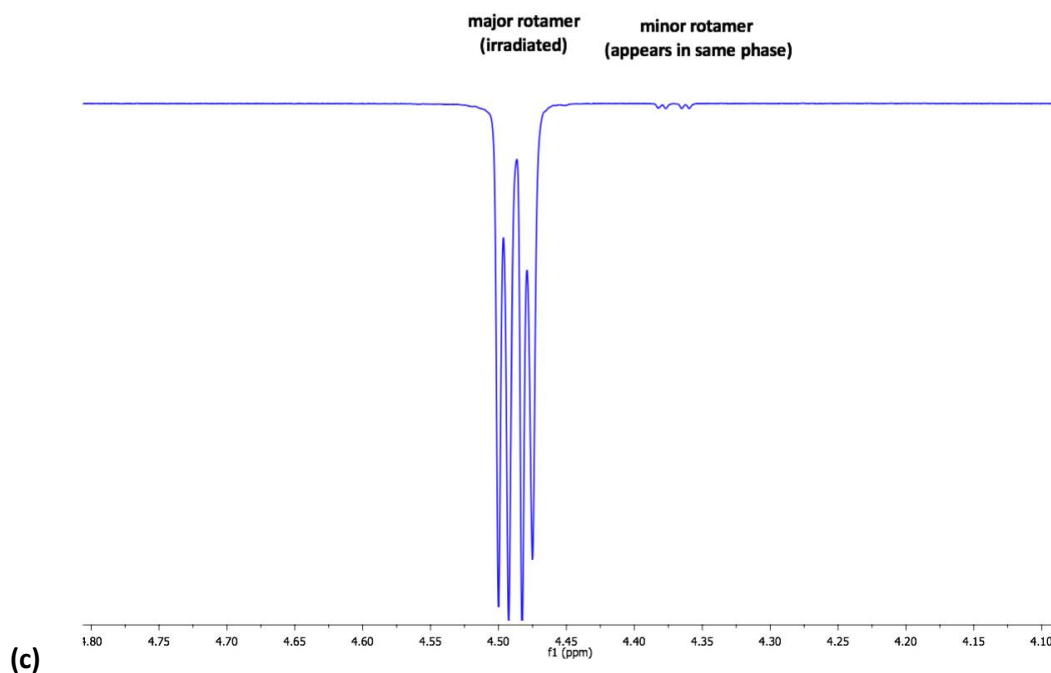


Figure 16. (a) ^1H NMR spectrum of Ac-Pro-OEt. Two NMR resonances are observed for each proton corresponding to the major and minor isomers. (b) 1D NOE spectrum of Ac-Pro-OEt. Selective excitation of the minor isomer at 4.37 ppm resulted in a peak of the *same* phase at 4.47 ppm due to isomeric chemical exchange (major isomer). (c) 1D NOE spectrum of Ac-Pro-OEt. Selective excitation of the signal of the major isomer at 4.47 ppm resulted in a new peak of the *same* phase at 4.37 ppm due to isomeric chemical exchange (minor isomer).

Different $K_{trans/cis}$ ratios were observed for the three proline analogs in solvents of different polarity at 85 nM. The major and minor isomers of *N*-(Acetyl)-proline **2.18**, *cis*-Ac-MPro-OEt **2.21**, and *trans*-Ac-MPro-OEt **2.22** were identified using NOESY 1D spectroscopy by selective excitation of the α ($\text{C}_i^\alpha - \text{H}$) proton. The *cis*-amide conformation exhibited NOE between the signals of the acetyl methyl protons ($\text{C}_{i-1}^\alpha - \text{H}$) and the α ($\text{C}_i^\alpha - \text{H}$) proton (Figure 17a). The *trans*-amide conformer showed NOE between the signals of the α ($\text{C}_i^\alpha - \text{H}$) proton ($\text{C}_{i-1}^\alpha - \text{H}$) and the β ($\text{C}_i^\beta - \text{H}$) (Figure 17b) indicating that the acetyl methyl protons ($\text{C}_{i-1}^\alpha - \text{H}$) are not in the vicinity (Figure 17b).

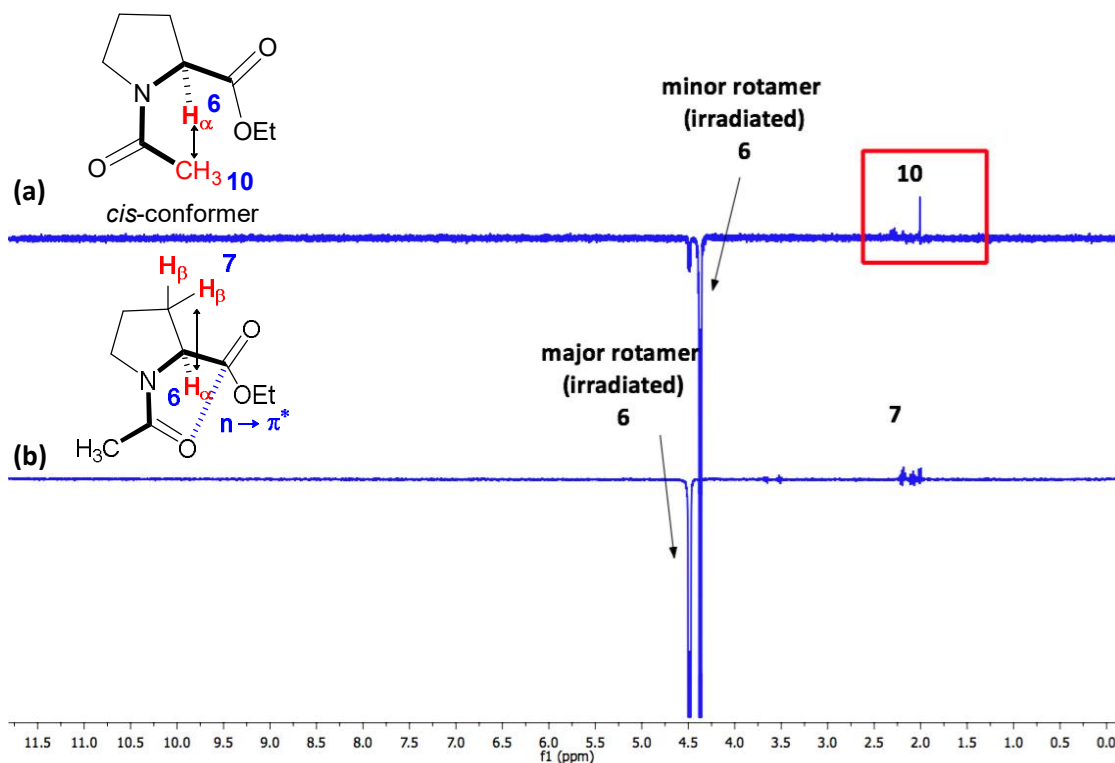


Figure 17. (a) 1D NOE spectrum of Ac-Pro-OEt **2.18**. Selective excitation of the minor isomer (6) at 4.37 ppm resulted in a peak at 2.00 ppm corresponding to the acetyl methyl protons ($C_{i-1}^{\alpha} - H$). Thereby, the minor isomer corresponds to the *cis*-amide conformer. **(b)** 1D NOE spectrum of Ac-Pro-OEt. Selective excitation of the major isomer 6 at 4.47 ppm resulted in peaks at 2.23-1.97 ppm corresponding to the β ($C_i^{\beta} - H$) protons. Thereby, the major isomer corresponds to the *trans*-amide conformer.

N-(Acetyl)-proline **2.18** and its methanoproline congeners **2.21** and **2.22** exhibited different isomer ratios in CDCl₃, C₆D₆, D₂O and DMSO (Figure 18). The *trans*-amide isomer dominated in all three congeners with *trans* : *cis* ratios ranging from 3 to 19. The observed isomer populations for *N*-(Acetyl)-proline **2.18** had ratios ranging from 3 to 5, and were in good agreement with the reported studies conducted by Raines and Wennemers.^{18, 20} The observed $K_{trans/cis}$ ratios for the *cis*-Ac-MPro-OEt **2.21** and *trans*-Ac-MPro-OEt **2.22** were higher than the *N*-(Acetyl)-proline **2.18**. Interestingly, the *trans*-Ac-MPro-OEt **2.22** turned out to have the most abundant *trans*-amide conformer. The observed $K_{trans/cis}$ ratios for

trans-Ac-MPro-OEt **2.22** range from 9 to 19, having twice the values of the *cis*-methano congener **2.21** and three times that of the natural proline derivative **2.18** (Figure 18). The methylene bridge favors the *trans*-amide isomer. The stereochemistry of the methylene bridge as well as the nature of the solvent, both affect the conformational equilibrium of the amide.

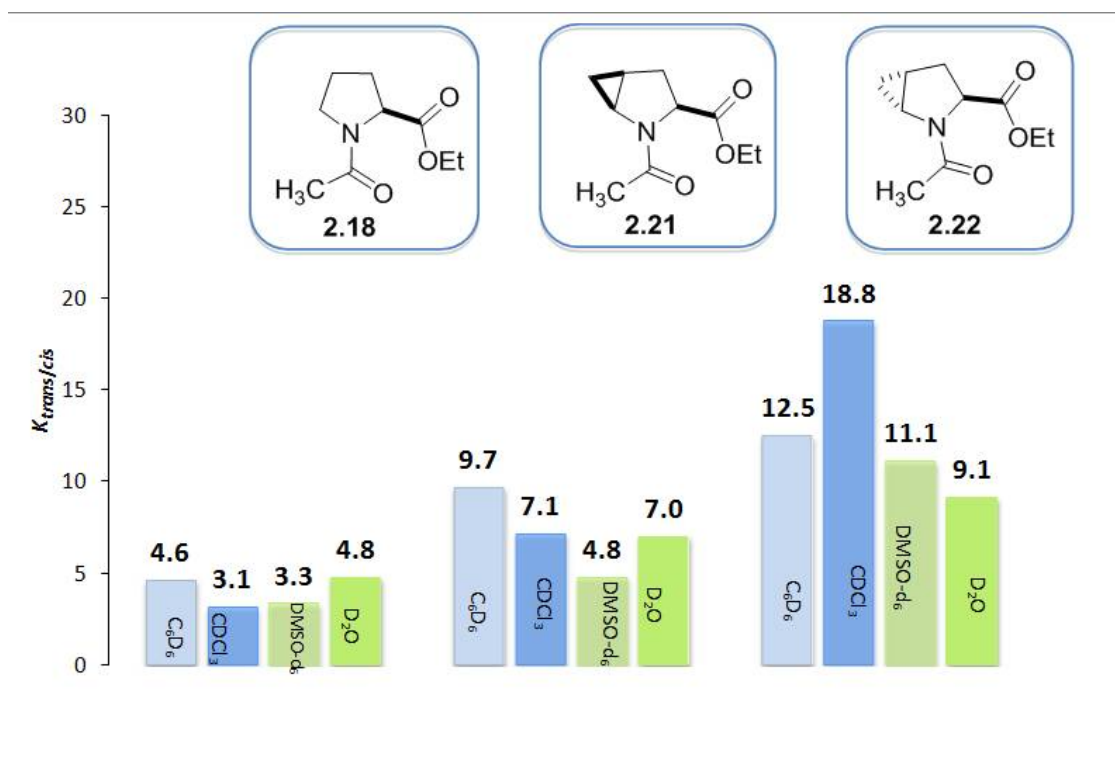


Figure 18. $K_{trans/cis}$ values of Ac-Pro-OEt, *cis*-Ac-MP-OEt, *trans*-Ac-MP-OEt obtained from the NMR-spectroscopy studies of 85 mM solutions in C_6D_6 , $CDCl_3$, $DMSO-d_6$, and D_2O . The Ac-Pro-OEt **2.18** resulted in the lowest $K_{trans/cis}$. Although DFT calculations resulted in the *cis*-Ac-MP-OEt **2.21** to have the highest $K_{trans/cis}$, this was not the case in the results obtained from the experiments conducted as the *trans*-Ac-MP-OEt **2.22** resulted in the highest $K_{trans/cis}$ ratio.

The $n \rightarrow \pi^*$ interaction is an important parameter that influences the stability of the *trans*-amide conformation. Through DFT calculations conducted by Dr. Gilles Berger, the relative free energies between the *cis*- and *trans*-amide conformations of the three compounds **2.18**, **2.21** and **2.22** were obtained in the gas phase.²⁸ As previously mentioned, the shorter the bond distance between the donor amide oxygen to the acceptor ester carbonyl, the stronger the $n \rightarrow \pi^*$ interaction. The *cis*-Ac-MPro-OEt **2.21** resulted in the highest calculated $n \rightarrow \pi^*$ stabilization (1.3 kcal/mol), followed by *N*-(Acetyl)-proline **2.18** (0.6 kcal/mol) and *trans*-Ac-MPro-OEt **2.22** (0.2 kcal/mol).²⁸ The discrepancy between the experimental $K_{trans/cis}$ ratio and the theoretical isomerization energies indicate that even though the strength of the $n \rightarrow \pi^*$ interaction influences the $K_{trans/cis}$ ratios, other factors such as solvent effects and steric hindrance also influence the *trans*-amide stabilization.

Kinetic and Conformational Studies of Diketopiperazine Formation

During the synthesis of oligomeric *cis*-4,5-methano-L-prolines, the free amine dipeptide ethyl ester **2.24** cyclized to form diketopiperazine (DKP) **2.28** (Figure 19). Diketopiperazines play important roles in neurophysiological function, and have certain applications in fossil analysis and thermal food processing.²⁹ Thus, a great deal of studies have been conducted to determine the mechanism of formation and the various factors affecting the cyclization process. The mechanism of the intramolecular cyclization involves the nucleophilic attack of the amine nitrogen in **2.24** onto the ester carbonyl group of the second amino acid. This highlights the equilibrium between the *cis*- and *trans*-conformations of the amide bond, as only the *cis*-conformation can enable the attack of the basic nitrogen on the ester carbonyl.

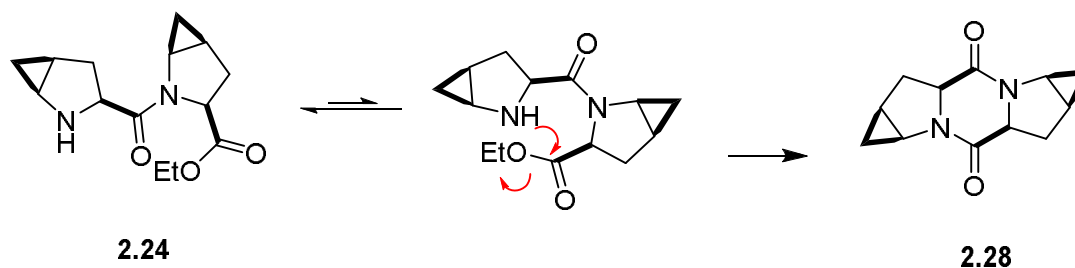
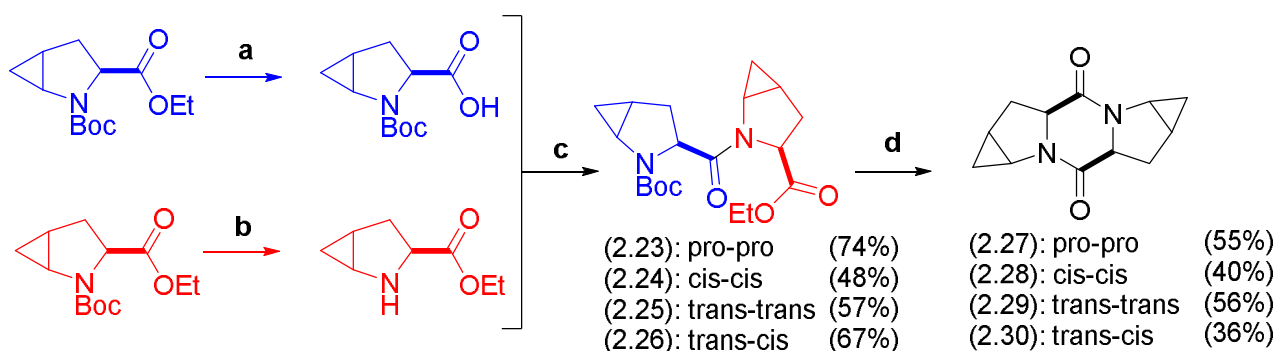


Figure 19. Cyclization of free amine *cis*-4,5-methano-L-proline ethyl ester dimer to a diketopiperazine.

Previously, de Mieijere and coworkers studied the cyclization of 3,4-(aminomethano)proline.²⁵ Although they were able to synthesize the first diketopiperazine made up of two 3,4-(aminomethano)proline subunits, the cyclization occurred in low yield due to the constraint introduced by the amino methylene bridge (Scheme 2).²⁵ Moreover, the Wennemers group synthesized previously diketopiperazines and cyclic triprolines. In this study, they highlighted the influence of the gauche effect in diastereomeric 4-azidoproline, in which the azido group alters ring puckering and amide isomer conformation.³⁰ With the diastereomeric 4,5-methano-L-proline monomers in hand, we studied their propensity to cyclize to the corresponding DKPs.

The monomeric *cis*- and *trans*-4,5-methano-L-proline were used to prepare the *cis-cis* **2.24**, *trans-trans* **2.25**, and *trans-cis* **2.26** dimers. The basic coupling procedure involves a free acid methanoproline monomer that is activated using 1-ethyl-3-(3-dimethylaminopropyl)carbodiimide (EDC) and hydroxybenzotriazole (HOBT), then coupled to the free amine proline ethyl ester derivative (Scheme 6). The rates of cyclization were monitored using ¹H NMR time-lapse experiments and TLC at varying temperatures.



Scheme 6. (a) LiOH, H₂O:MeOH, 86% (4:1) rt. (b) TFA, DCM, 0° C; 60-90 min 93%. (c) EDC.HCl, HOBT, DIPEA, DCM, r.t 40-60%. (d) TFA, DCM, 0° C; 60-90 min, 30-60%.

The ^1H NMR spectra were recorded at regular time intervals times at room temperature and 40 °C. The starting material H α 1 proton signal intensity should decrease while the product H α 2 proton signal intensity increases (Figure 20). The *pro-pro* dimer **2.23** was the fastest to cyclize giving diketopiperazine **2.27** in 18 h at 25 °C (Figure 21a). The cyclization of *trans-trans* diastereomer **2.29** was complete in 68 h at 40 °C followed by those of *trans-cis* **2.30** and *cis-cis* **2.28**, which cyclized in 9 days and 15 days at 40 °C, respectively (Figure 21b, c, d).

Cyclization experiments were also conducted at 60 °C, and monitored at regular intervals by thin layer chromatography (TLC). The same trend in cyclization rates was observed for the diketopiperazine formation of all four dimers, albeit at higher temperature, *trans-* to *cis-*amide isomerization, and cyclization occurred faster. The *pro-pro* **2.23** cyclized the fastest within 30 mins, followed by the *trans-trans* **2.25** which was complete within an hour. The *trans-cis* **2.26** and *cis-cis* **2.24** cyclized within 3 h and 5 h, respectively.

These results agreed with the theoretical data reported by our group. The NBO analyses revealed stronger $n \rightarrow \pi^*$ interactions in the *cis*-4,5-methanoproline dimer **2.24** congener, which stabilize the *trans*-amide conformation leading to a slower *trans* to *cis*-amide conversion,¹⁷ which should in turn slow cyclization to the diketopiperazine. On the other hand, the *trans*-4,5-methanoproline dimer **2.25** congener lacks efficient $n \rightarrow \pi^*$ interaction due to improper overlap between the amine lone pair and the ester carbonyl.¹⁷ Based on the Curtin-Hammett principle, it is assumed that the intramolecular cyclization is of first-order kinetics in which the rate of the reactions is dependent solely on the *cis-* to *trans-* isomerization ratio and concentration of the *cis*-amide conformer.

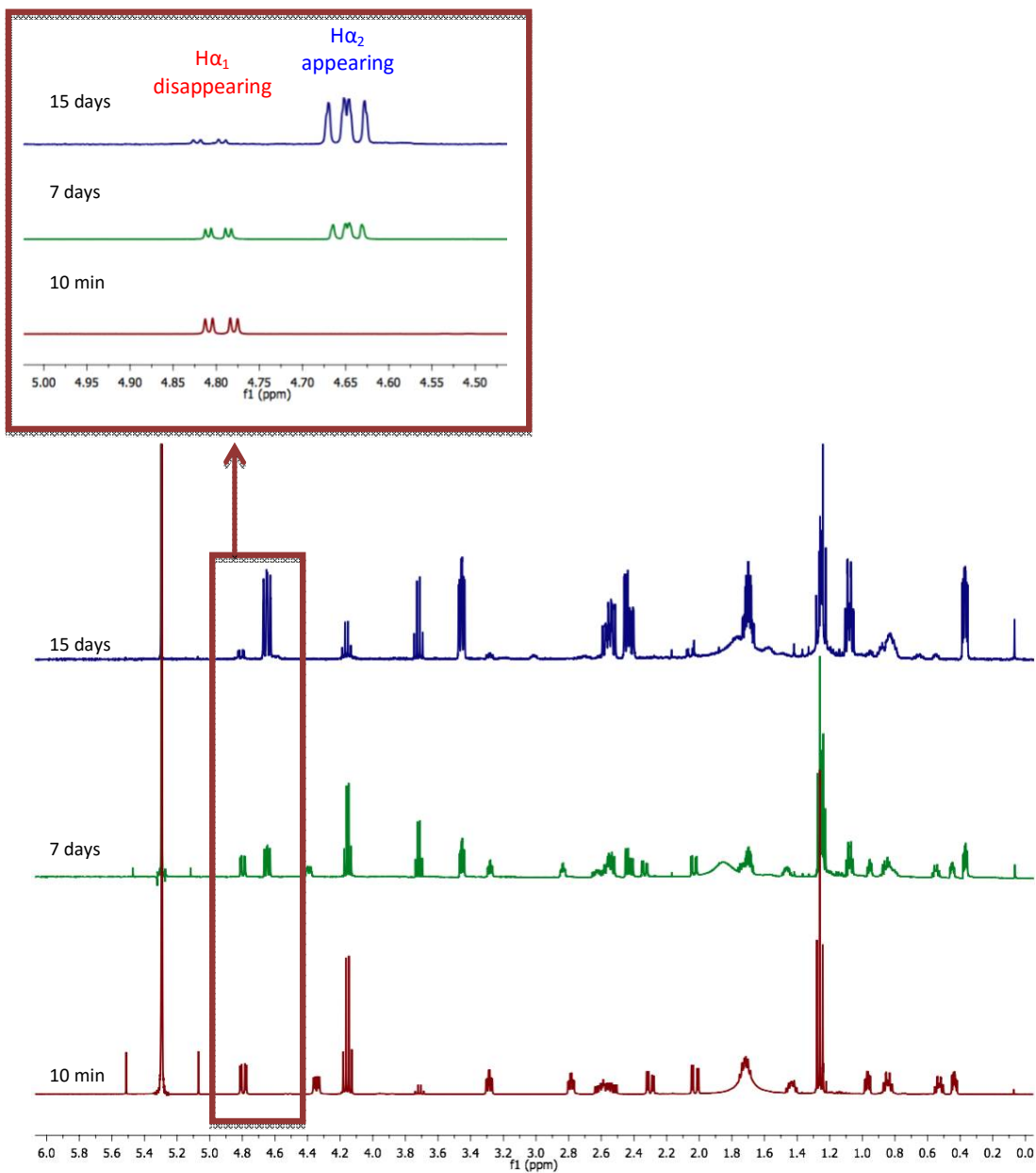
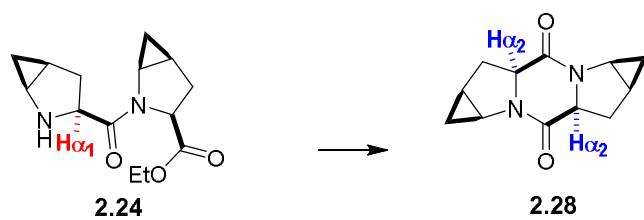
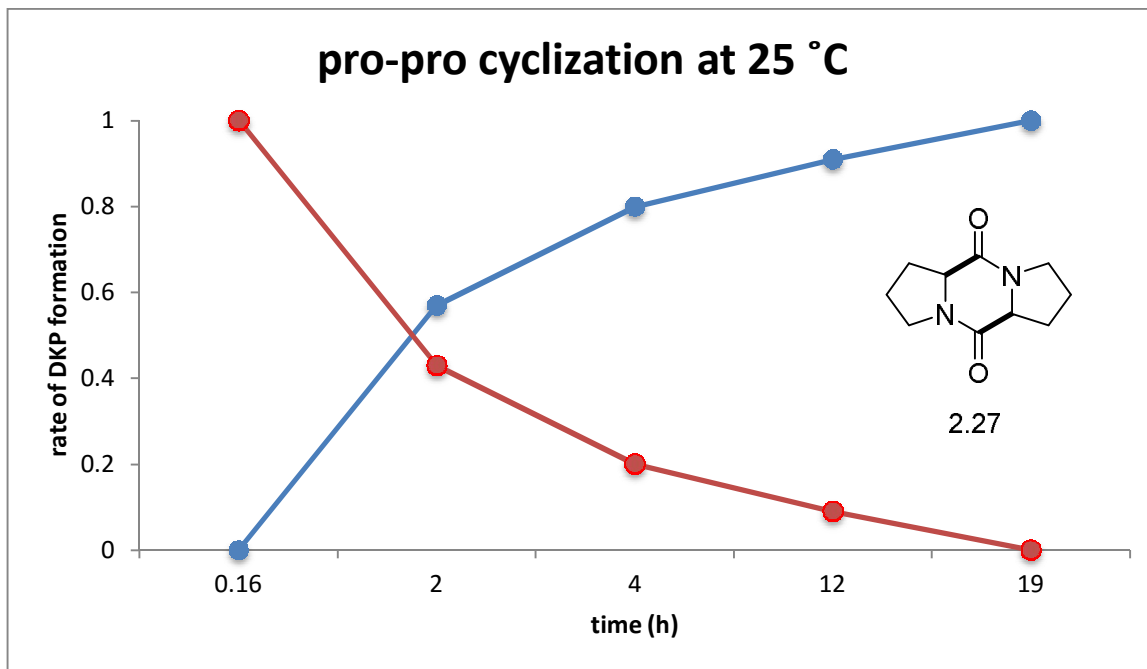
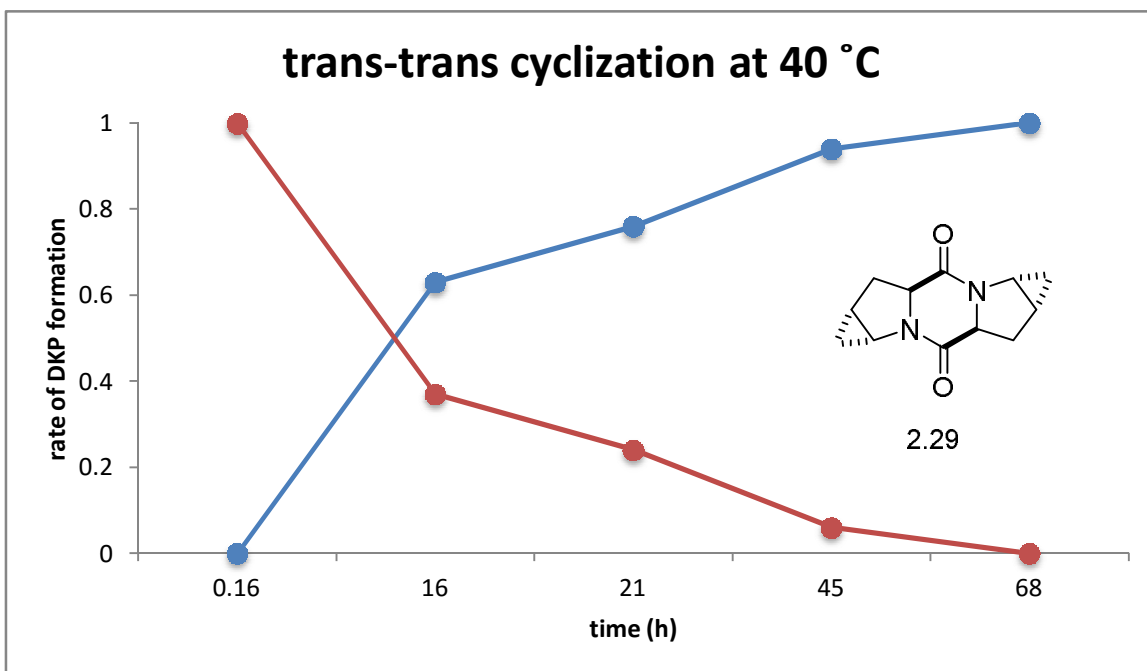


Figure 20. ^1H NMR time lapse of the *cis-cis* **2.24** free amine dimer cyclization to the diketopiperazine **2.28** at 40 °C. The $\text{H}\alpha_1$ proton of the starting material at 4.80 ppm is disappearing overtime while the $\text{H}\alpha_2$ proton of the diketopiperazine is appearing at 4.65 ppm.

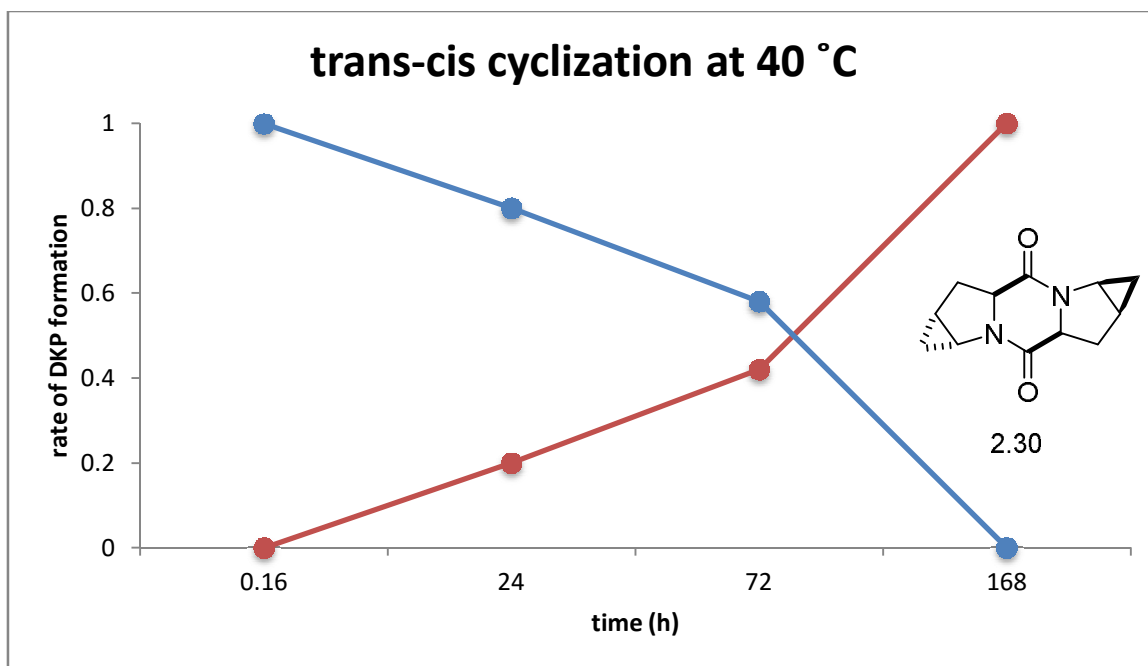
(a)



(b)



(c)



(d)

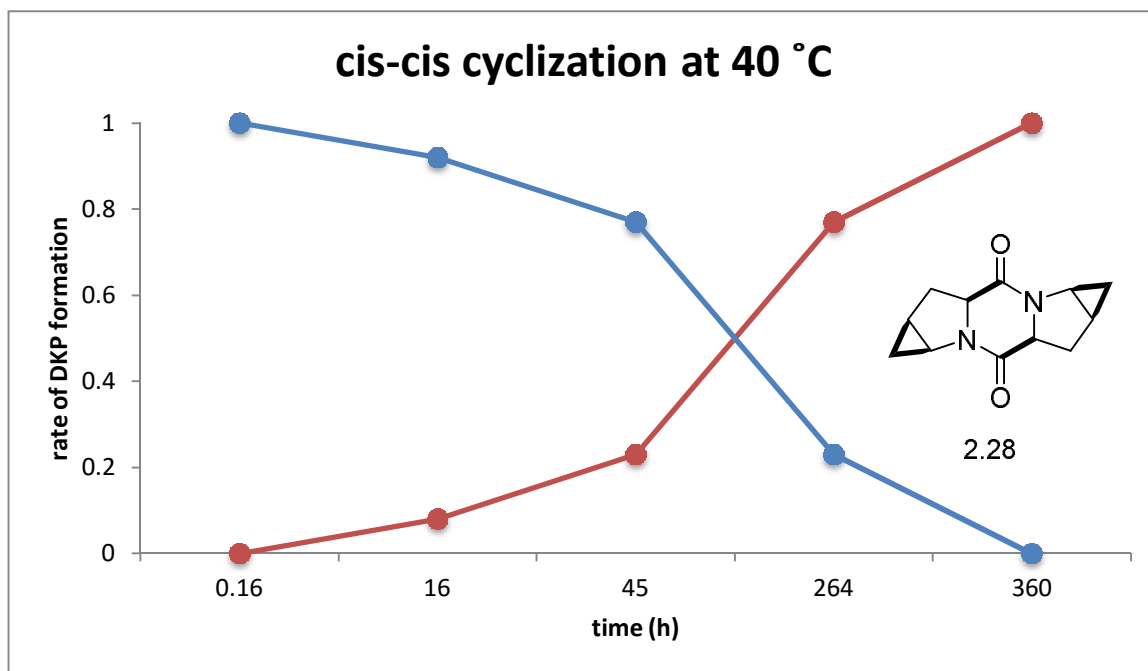


Figure 21. Rate of diketopiperazine formation of: *pro-pro* 2.25 at 25 °C, *trans-trans* 2.27, *trans-cis* 2.28 and *cis-cis* 2.26 at 40 °C.

Conclusion

Using ^1H NMR spectroscopy we determined that the *trans*-amide conformer was dominant in all proline analogs regardless of the solvent. The *trans*-Ac-MP-OEt possesses the highest $K_{trans/cis}$, followed by *cis*-Ac-MP-OEt and *N*-(Acetyl)-proline. However, these results do not correlate with the NBO studies which predicted the *cis*-Ac-MP-OEt to have the most stable $n \rightarrow \pi^*$ interaction. This discrepancy highlights the effects imposed by environment.

The cyclization of the dimeric *pro-pro*, *trans-trans*, *trans-cis*, and *cis-cis* analogs to the corresponding diketopiperazines were achieved. The presence of the cyclopropane ring may impose steric effects on the pyrrolidine ring. The rates of cyclization proved to be dependent on the stereochemistry. The *trans-trans* analog cyclized the fastest, followed by the *trans-cis* and *cis-cis*. These results correlated with the previously calculated values for the *trans*- to *cis*-amide isomerization ratios.

The combined experimental and theoretical analysis presented in this thesis provide an understanding of the conformational properties of *cis*- and *trans*-4,5-methano-L-prolines. The experimental results show that the steric hindrance introduced by the methylene bridge and the polarity of the environment affect $n \rightarrow \pi^*$ electron stabilization, in turn influencing the $K_{trans/cis}$ ratio of each proline derivative.

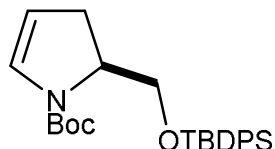
Experimental Notes

All non-aqueous reactions were run in oven-dried glassware under argon. Anhydrous solvents were obtained using standard drying techniques. Unless stated otherwise, commercial grade reagents were used without further purification. Reactions were monitored by TLC on pre-coated, glass-backed silica gel plates. Visualization of the developed chromatogram was performed by UV absorbance, aqueous cerium ammonium molybdate, aqueous ninhydrin, iodine, or aqueous potassium permanganate. Flash chromatography was performed on 230-400 mesh silica gel with the indicated solvent systems. Routine nuclear magnetic resonance spectra were recorded either on a Bruker AV-400 or AV-500 spectrometer. Chemical shifts for ^1H NMR spectra are recorded in parts per million from tetramethylsilane (TMS) with the solvent resonance CHCl_3 (δ 7.26) and DMSO-d_6 (δ 2.50) or TMS (δ 0.00) as the internal standard. Data are reported as follows: chemical shift, integration, multiplicity (s = singlet, d = doublet, t = triplet, q = quartet, qn = quintet, m = multiplet and br = broad), and coupling constant in Hz. Chemical shifts for ^{13}C NMR spectra are recorded in parts per million from tetramethylsilane using the central peak of the solvent resonance as the internal standard (CDCl_3 , δ 77.0) and DMSO-d_6 (δ 39.51). All ^{13}C spectra were obtained with complete proton decoupling. Optical rotations were determined at 589 nm and room temperature. Data are reported as follows: $[\alpha]_{\text{D}}^{20}$, solvent and concentration (c in g/100 mL). High-resolution mass spectrometry was performed by the "Centre régional de spectroscopie de masse de l'Université de Montréal" using electrospray ionization (ESI) coupled to quantitative time-of-flight detection.

Experimental Procedures

1. Synthesis of *trans*-4,5-methano-L-proline²⁷

1.1 - *tert*-Butyl (*S*)-2-(((*tert*-butyldiphenylsilyl)oxy)methyl)-2,3-dihydro-1*H*-pyrrole-1-carboxylate (**2.14**)²⁷

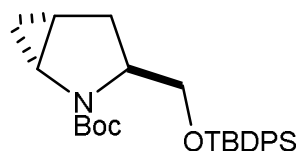


Chemical Formula: C₂₆H₃₅NO₃Si
Molecular Weight: 437.66

Boc-pGlu-OTBDPS **2.13** (8 g, 17.6 mmol) was dissolved in toluene (30 mL) in a flame-dried three-necked flask equipped with a thermometer and a nitrogen inlet. The temperature of the solution was lowered to -55 °C using an acetone cooling bath. Once the internal temperature of the solution reached -55 °C, superhydride (21 mL of 1.0 M in THF, 21.1 mmol) was added dropwise over 30 min, and the mixture was followed by TLC at -55 °C. DIPEA (13.2 mL, 75.7 mmol) was added dropwise over 10 min. DMAP (21 mg, 0.176 mmol) was added in one batch, followed by the slow addition of TFAA (1.55 mL, 20.2 mmol) while maintaining the temperature between -55 °C and -45 °C. After 10 min, the reaction mixture was warmed to room temperature and allowed to stir overnight. The mixture was diluted with toluene (10 mL) and cooled with an ice-water bath. Water (55 mL) was added slowly over 5 mins. The phases were separated and the collected organic layer was washed twice with water (50 mL), dried over Na₂SO₄ and evaporated under reduced pressure. The crude material was purified by flash chromatography (silica gel; 5% EtOAc/hexane) to afford the ene-carbamate **2.14** as a pale yellow oil (6.8 g, 88% yield).

¹H NMR (400 MHz, CDCl₃, δ = 7.26) δ 7.71-7.55 (m, 4H), 7.46-7.32 (m, 6H), 6.50 (d, *J* = 44.0 Hz, 1H), 4.97 (d, *J* = 32.4 Hz, 1H), 4.25 (d, *J* = 41.9, 1H), 3.92 (br s, 0.5H), 3.82-3.73 (m, 1H), 3.66 (d, *J* = 7.4 Hz, 0.5H), 2.78 (br m, 2H), 1.53-1.22 (overlapping s, 9H), 1.06 (s, 9H). ¹³C NMR (400 MHz, CDCl₃, δ = 77.0 ppm) δ 152.2, (151.7 minor Boc conformer), 135.7, 133.8, 129.4, 127.9, 107.1, (106.8 minor Boc conformer), 80.2, (80.0 minor Boc conformer), 64.1, 58.6, (58.1 minor Boc conformer) 33.5, (32.5 minor Boc conformer), 28.5, (28.4 minor Boc conformer), 26.9, 19.5. LC/MS: [M+Na]⁺ = 460.1902

1.2 - *tert*-Butyl (1*R*,3*S*,5*R*)-3-(((*tert*-butyldiphenylsilyl)oxy)methyl)-2-azabicyclo[3.1.0]hexane-2-carboxylate (2.15)²⁷

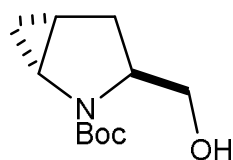


Chemical Formula: C₂₇H₃₇NO₃Si
Molecular Weight: 451.68

Dihydropyrrole **2.14** (4 g, 9.14 mmol) was dissolved in toluene (30 mL) in a flame-dried three-necked flask equipped with a thermometer and a nitrogen inlet. The temperature of the solution was lowered to -35 °C using an acetonitrile cooling bath. Once the internal temperature of the solution reached -35 °C, diethylzinc (21 mL of 1.0M/THF, 20.0 mmol) was added dropwise over 15 min while maintaining the temperature at -25 °C. Chloriodomethane (stabilized over copper; 3.06 mL, 42.0 mmol) was added dropwise over 10 min with stirring while maintaining the bath temperature at -25 °C for 1 h and between -25 °C and -21 °C for 18.5 h. The reaction mixture was then opened to air and quenched with a 50% saturated NaHCO₃ solution (40 mL) and stirred at room temperature for 20 min. The mixture was filtered through celite and the white cake was washed with 50 mL of toluene. The organic phase was then collected and washed with water (40 mL, 2x), dried over Na₂SO₄, and concentrated *in vacuo*. The residue was purified by flash chromatography (silica gel; 3% EtOAc/hexane) to afford a stereoisomeric mixture of Boc-methano-L-proline-OTBDPS **2.15**, mainly the *trans* isomer, as a colorless oil (3.6 g, 87% yield). [Note: the exact ratio of the *trans*- and *cis*- stereoisomers has not been determined yet at this stage.]

¹H NMR (500 MHz, CDCl₃, δ = 7.26) δ 7.69-7.64 (m, 4H), 7.51- 7.31 (m, 6H), 3.87 (overlapping br s, 1H), 3.72 (d, *J* = 5.4 Hz 2H), 3.2 (br s, 1H), 2.34 (s, 1H), 2.18-1.94 (m, 1H), 1.61-1.50 (m, 1H) 1.49-1.24 (very broad s, 9H), 1.07 (s, 9H), 0.86 (m, 1H), 0.29 (m, 1H). ¹³C NMR (500 MHz, CDCl₃, δ = 77.0 ppm) δ 155.8, 135.6, 133.7, 129.6, 127.7, 79.4, 65.2, 62.7, 53.4, 37.1, 28.5, 26.8, 19.4, 18.6. LC/MS: [M+Na]⁺ = 474.141.

1.3 - *tert*-Butyl (1*R*,3*S*,5*R*)-3-(hydroxymethyl)-2-azabicyclo[3.1.0]hexane-2-carboxylate (**2.16**)²⁷

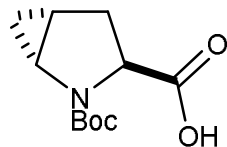


Chemical Formula: C₁₁H₁₉NO₃
Molecular Weight: 213.28

TBAF (7.0 mL of 1.0 M in THF, 6.0 mmol) was added dropwise to a solution of silyl ether **2.15** (3.0 g, 6.64 mmol) in THF (30 mL). The mixture was stirred at room temperature for 4.75 h. The reaction was quenched by the addition of saturated NH₄Cl solution (5 mL). The volatiles were evaporated *in vacuo*. The residue was partitioned between CH₂Cl₂ (70 mL) and 50% saturated NH₄Cl solution (30 mL). The aqueous phase was extracted with CH₂Cl₂ (30 mL). The combined organic layer was dried over Na₂SO₄. The volatiles were evaporated under reduced pressure, and the residue was left on high vacuum overnight. The crude product was purified by flash chromatography (silica gel; 40-50% EtOAc/hexane) to afford a stereoisomeric mixture of alcohols **2.16**, mainly the *trans* isomer as a colorless oil, contaminated with traces of a lower R_f spot (1.27 g, 90% yield). [Note: Note: the exact ratio of the *trans*- and *cis*-stereoisomers has not been determined yet at this stage.]

¹H NMR (500 MHz, CDCl₃, δ = 7.26) δ 4.91 (br s, 1H), 3.68 (m, 1H), 3.58 (d, *J* = 5.6 Hz 2H), 3.24 (td, *J* = 6.5, 2.4 Hz, 1H), 2.12 (dd, *J* = 13.2, 8.3 Hz, 1H), 1.75 (br s, 2H), 1.51-1.42 (s, 9H), 0.70 (br s, 1H), 0.38 (td, *J* = 5.3, 2.4 Hz, 1H). ¹³C NMR (500 MHz, CDCl₃, δ = 77.0 ppm) δ 158.6, 80.65, 67.01, 61.34, 37.63, 31.04, 28.54, 28.17, 14.63. LC/MS: [M+Na]⁺ = 236.2054

1.4 - *trans*-Boc-4,5-Methano-L-proline carboxylic acid or (1*R*,3*S*,5*R*)-2-(*tert*-butoxycarbonyl)-2-azabicyclo[3.1.0]hexane-3-carboxylic acid (2.6)



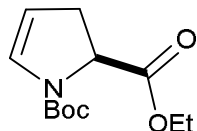
Chemical Formula: C₁₁H₁₇NO₄
Molecular Weight: 227.26

A three-necked flask was charged with alcohol **2.16** (0.85 g, 4.0 mmol), TEMPO (2,2,6,6-tetramethyl-1-piperidinyloxy free radical) (0.04 g, 0.28 mmol), 50 mL of acetonitrile and 15 mL of 0.67 M sodium phosphate buffer (pH 4). The reaction mixture was heated at 35 °C. A solution of dilute sodium hypochlorite (NaOCl) was prepared by the addition of (5.25% NaOCl, 0.011 mL) to 1.9 mL of water, and a solution of sodium chlorite was prepared by dissolving 80% NaClO₂ (0.9 g, 8.0 mmol) in 4 mL of water. Once target temperature of reaction mixture was attained, approximately 20% of the prepared NaClO₂ solution was added using an addition funnel followed by 20% of dilute bleach solution via a second addition funnel. The remaining portions of both reagents were then added simultaneously dropwise over 2 h. The reaction mixture was stirred vigorously overnight and tracked by TLC until completion. The mixture was allowed to cool to room temperature, treated with 30 mL of water, and the pH was adjusted to 8.0 by the addition of 2.0 N NaOH. The mixture was then added to an ice-cold solution of sodium sulfite (1.2 g in 20 mL of water) and stirred below 20 °C for 30 minutes. Ethyl acetate was then added and the resulting mixture was stirred for another 15 min. The pH was acidified to 3-4 with 2 N HCl, the layers were separated and the aqueous layer was extracted with EtOAc (25 mL, 2x). The combined organic phase was then washed with water (25 mL, 2x), dried over Na₂SO₄ and concentrated under reduced pressure to obtain a white solid. The crude material was purified by crystallization at room temperature using a minimal amount of warm EtOAc followed by the slow addition of hexane. First crop (0.54 g, 60% yield). Second crop (0.25 g, 27% yield).

¹H-NMR (500 MHz, DMSO-D₆, δ = 2.50 ppm) δ 12.46 (s, 1H), 3.88 (app br s, 1H), 3.27 (app br s, 1H; overlapped with water signal), 2.28 (br m, 1H), 2.07 (app br s, 1H), 1.56 (app s, 1H), 1.40/1.34 (two overlapped s, 9H), 0.71 (m, 1H), 0.45 (m, 1H). **¹³C-NMR** (500 MHz, DMSO-D₆, δ = 39.21 ppm) δ 173.6, (172.9 minor conformer), 154.5, (153.9 minor conformer), 78.8, 60.8, (59.7 minor conformer), 37.1, 31.97, (31.3 minor conformer), 27.9, (27.4 minor conformer), 14.8, (14.3 minor conformer), 13.6. LC/MS [M+Na]⁺ = 250.2201

2. Synthesis of *cis*-4,5-methano-L-proline

2.1 - 1-(*tert*-Butyl) 2-ethyl (S)-2,3-dihydro-1*H*-pyrrole-1,2-dicarboxylate (**2.10**)^{11, 26-27}

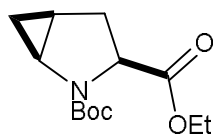


Chemical Formula: C₁₂H₁₉NO₄
Molecular Weight: 241.29

Boc-pGlu-OEt **2.9** (1.29 g, 5.0 mmol) was dissolved in toluene (10 mL) in a flame-dried three-necked flask equipped with a thermometer and a nitrogen inlet. The temperature of the solution was lowered to -78 °C using an acetone cooling bath. Once the internal temperature of the solution reached -78 °C, Super-Hydride (5.3 mL of 1.0 M in THF, 5.3 mmol) was added dropwise over 30 min, and the mixture was stirred at -78 °C for 2 h. DIPEA (5.0 mL, 28.5 mmol) was added dropwise over 10 min. DMAP (12 mg, 0.1 mmol) was added in one batch, followed by the slow addition of TFAA (0.85 mL, 6.0 mmol) while maintaining the temperature between -78 °C and -73 °C. After 10 min, the reaction mixture was warmed to room temperature and allowed to stir overnight. The mixture was diluted with toluene (10 mL) and cooled with an ice-water bath. Water (10 mL) was added slowly over 5 mins. The phases were separated and the collected organic layer was washed with water (10 mL, 2x), dried over Na₂SO₄ and evaporated under reduced pressure. The crude material was purified by flash chromatography (silica gel; 5% EtOAc/hexane) to afford ene-carbamate ethyl ester **2.10** as yellow oil (1.11 g, 92% yield).

¹H NMR (500 MHz, CDCl₃, δ = 7.26) δ 6.56-6.43 (m, 1H), 4.87-4.82 (m, 1H), 4.57-4.46 (m, 1H), 4.20-4.08 (m, 2H), 3.09-2.89 (m, 1H), 2.67-2.49 (m, 1H), 1.37 (s, 9H), 1.26-1.13 (m, 3H). ¹³C NMR (500 MHz, CDCl₃, δ = 77.0 ppm) δ 171.8, (171.5 minor conformer), 151.3, 129.9, 104.9, 80.7, 61.1, (60.2 minor conformer) 58.35, (57.88 minor conformer), 35.42, (34.25 minor conformer), 28.2, (28.1 minor conformer), 14.2, (14.0 minor conformer). LC/MS: [M+Na]⁺ = 264.1212

2.2 - *cis*-Boc-4,5-methano-L-proline ethyl ester or 2-(*tert*-Butyl) 3-ethyl (1*S*,3*S*,5*S*)-2-azabicyclo[3.1.0]hexane-2,3-dicarboxylate (2.12)



Chemical Formula: C₁₃H₂₁NO₄
Molecular Weight: 255.31

Dihydropyrrole ethyl ester **2.10** (0.9 g, 3.7 mmol) was dissolved in toluene (13 mL) in a flame-dried three-necked flask equipped with a thermometer and a nitrogen inlet. The temperature of the solution was lowered to -35 °C using an acetonitrile cooling bath. Once the internal temperature of the solution reached -35 °C, diethylzinc (8.1 mL of 1.0M/THF, 8.1 mmol) was added dropwise over 15 min while maintaining the temperature at -25 °C. Chloriodomethane (stabilized over copper; 1.24 mL, 17.02 mmol) was added dropwise over 10 min, and stirred while maintaining the bath temperature at -25 °C for 1 h and between -25 °C and -21 °C for 18.5 h. The reaction mixture was opened to air and quenched with 50% saturated NaHCO₃ solution (15 mL) and allowed to stir at room temperature for 20 min. The mixture was filtered through celite, and the white cake was washed with 20 mL of toluene. The organic phase was collected and washed with water (15 mL, 2x), dried over Na₂SO₄, and concentrated *in vacuo*. The residue was purified by flash chromatography (silica gel; 3% EtOAc/hexane) to afford a stereoisomeric mixture of Boc-4,5-methano-L-proline ethyl ester **2.12**, mainly the *cis* doastereomer in a 11:1 ratio, as pale yellow oil (0.86 g, 91% yield).

¹H NMR (500 MHz, CDCl₃, δ = 7.26) δ 4.45(dd, *J* = 11.5, 3.1 Hz, 0.3, minor Boc conformer) and 4.46(dd, *J* = 11.5, 3.3 Hz, 0.7H, major Boc conformer), 4.21-3.98 (m, 2H), 3.50 (td, *J* = 6.3, 2.5 Hz 0.7H, major Boc conformer), 3.41 (td, *J* = 6.3, 2.5, 1H, minor Boc conformer), 2.68-2.41 (m, 1H), 1.51-1.42 (2 s, 9H, rotamers), 1.21(m, 3H), 0.85 (m, 1H), 0.76–0.56 (m, 1H). ¹³C NMR (500 MHz, CDCl₃, δ = 77.0 ppm) δ 173.6, (173.3 minor conformer), (154.4 minor conformer), 154.2, 80.0, 61.0, (60.4 minor conformer), 59.8, (59.3 minor conformer), 37.3, (37.1 minor conformer), 31.8, (30.6 minor conformer), (28.4 minor conformer), 28.3, (15.4 minor conformer), 15.2, 14.4, (14.0 minor conformer), 12.9, (12.4 minor conformer). **LC/MS:** [M+Na]⁺ = 278.1368

Synthesis of acetylated derivatives Ac-Pro-OEt 2.18, *cis*-Ac-MP-OEt 2.21, and *trans*-Ac-MP-OEt 2.22

(3) General Acetylation Procedure³¹

(3.1) Esterification

Carboxylic acid monomer **2.6** was dissolved in ethanol and the temperature was cooled to 0 °C. Thionyl chloride (1.1 eq) was added dropwise to the solution. The solution was stirred at room temperature and monitored by TLC. When complete, the volatiles were evaporated under reduced pressure, and the residue was left on a vacuum pump overnight and used in the acetylation procedure without further purification.

(3.2) Boc Deprotection

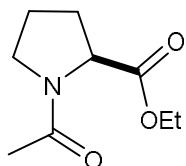
Carbamates proline (commercially available), **2.11**, and **2.12** were treated with TFA (10 eq) in dry dichloromethane (1 M) at 0 °C. The reaction was followed by TLC (60 to 90 min). The excess TFA was neutralized with saturated sodium bicarbonate. The layers were separated and the aqueous layer was extracted two times with dichloromethane. The combined organic layers were dried over Na₂SO₄ and used directly in the acetylation reaction with the activated acid, as described below.

(3.3) Acetylation

Acetyl chloride (1.2 eq) was added dropwise to a mixture of amine ethyl ester analogs and pyridine (1.2 eq) in THF (0.4 M) at 0 °C. The mixture was stirred for 1 h at 0 °C and for another 2 h at room temperature, poured into 2 N HCl at 0 °C, and extracted with EtOAc. The organic phase was washed with saturated NaHCO₃, dried over Na₂SO₄ and concentrated under reduced pressure to afford the acetylated derivatives. The crude product was purified by flash chromatography (silica gel; 30% EtOAc/hexane) to afford a white solid.

Ac-Pro-OEt 2.18

Ethyl acetyl-L-prolinate



Chemical Formula: C₉H₁₅NO₃
Molecular Weight: 185.22

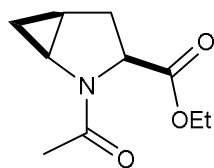
Following procedure 3.2 and 3.3 – 500 mg of *N*-Boc-Proline-OEt (2.06 mmol) gave 343 mg of ethyl acetyl-*L*-prolinate as a white solid.

¹H NMR (500 MHz, CDCl₃, δ = 7.26) δ 4.46 (dd, *J* = 8.6, 3.8 Hz, 0.8H), 4.34 (dd, *J* = 8.6, 2.7 Hz, 0.2H), 4.25-4.12 (m, 2H), 3.69-3.59 (m, 1H), 3.58-3.46 (m, 1H), 2.33-2.11 (m, 0.7H), 2.11-1.87 (m, 3.22H), 1.33-1.20 (m, 3H). ¹³C NMR (500 MHz, DMSO-d₆, δ = 77.0 ppm) δ 172.5, 168.7, 61.4, 60.7, 59.7, 58.5, 47.7, 46.2, 31.2, 29.4, 24.8, 22.8, 22.5, 14.5. FTIR (cm⁻¹, ATR) ν_{max} 1738, 1649, 1415, 1373, 1277, 1186, 1096, 1032 755. ESI-QTOF HRMS Calcd for C₉H₁₆NO₃ (MH⁺) 186.1102, found 186.1104. [α]_D²⁰ = -73.6° (CDCl₃, c = 10). Yield = 90%

cis-Ac-MP-OEt 2.21

Ethyl (1*S*,3*S*,5*S*)-2-acetyl-2-azabicyclo[3.1.0]hexane-3-carboxylate

Following procedure 3.2 and 3.3 – 350 mg of *N*-Boc-4,5-methano-*L*-proline-OEt **2.12** (1.37 mmol) gave 232 mg of *cis*-Ac-MP-OEt as a yellow oil.



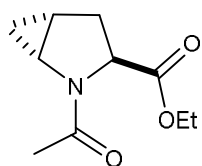
Chemical Formula: C₁₀H₁₅NO₃
Molecular Weight: 197.23

¹H NMR (500 MHz, CDCl₃, δ = 7.26) δ 4.74 (dd, *J* = 11.6, 3.5 Hz, 0.7H, major conformer), 4.55 (dd, *J* = 11.3, 2.4 Hz, 0.2H, minor conformer), 4.25-4.08 (m, 2H), 3.94 (td, *J* = 6.4, 2.5 Hz, 1H), 3.34 (ddd, *J* = 6.6, 5.9, 2.5 Hz, 1H), 2.72-2.63 (m, 0.2H, minor conformer), 2.63-2.53 (m, 0.7H, major conformer), 2.22 (s, 2.4H, major conformer), 2.02 (dd, *J* = 13.7, 3.6 Hz, 1H), 1.97 (s, 1H, minor conformer), 1.67 (ddd, *J* = 11.4, 9.1, 6.2 Hz, 2H), 1.31-1.22 (m, 4H), 1.11-1.04 (td *J* = 2.5, 2.5, 2.4 Hz), 0.85-0.78 (m, 1H). **¹³C NMR** (500 MHz, CDCl₃, δ = 77.0 ppm) δ 172.7, 169.4, 61.8, 61.1, 59.7, 38.1, 37.0, 32.1, 31.7, 30.3, 22.3, 17.4, 16.6, 14.1, 13.4, 11.5. **FTIR** (cm⁻¹, ATR) v_{max} 1738, 1644, 1418, 1371, 1189, 1096, 1032, 752, 664, 616. **ESI-QTOF HRMS** Calcd for C₁₀H₁₆NO₃ (MH⁺) 198.1104, found 198.1101. [α]_D²⁰ = -23.2 ° (CDCl₃, *c* = 10). Yield = 86%

trans-Ac-Mp-OEt 2.22

Ethyl (1*R*,3*S*,5*R*)-2-acetyl-2-azabicyclo[3.1.0]hexane-3-carboxylate

Following procedure 3.1, 3.2 and 3.3 – 350 mg of *trans*-*N*-Boc-4,5-methano-L-proline-OH **2.6** (1.5 mmol) gave 236 mg of *trans*-Ac-MP-OEt as a yellow-brown oil.



Chemical Formula: C₁₀H₁₅NO₃
Molecular Weight: 197.23

¹H NMR (500 MHz, CDCl₃, δ = 7.26) δ 4.36 (dd, *J* = 8.4, 5.8 Hz, 0.7H, major conformer), 4.27 (m, 2H), 3.38 (ddd, *J* = 7.0, 5.5, 2.5 Hz, 1H), 2.34-2.25 (m, 2H), 2.21 (s, 3H), 1.83-1.72 (m, 1H), 1.34-1.20 (m, 3H), 1.02-0.93 (m, 1H), 0.54 (td, *J* = 5.3, 2.5 Hz, 1H). **¹³C NMR** (500 MHz, CDCl₃, δ = 77.0 ppm) δ 171.6, 170.8, 61.6, 61.2, 38.2, 31.7, 29.7, 22.2, 18.3, 17.4, 14.1. **FTIR** (cm⁻¹, ATR) v_{max} 1742, 1654, 1418, 1345, 1274, 1190, 1112, 1030, 755. **ESI-QTOF HRMS** Calcd for C₁₀H₁₆NO₃ (MH⁺) 198.1102, found 198.1102. [α]_D²⁰ = -165 ° (CDCl₃, *c* = 10). Yield = 78%

Synthesis of *pro-pro*-L-proline dimer 2.23, *cis-cis* 2.24, *trans-trans* 2.25, and *trans-cis*-4,5-methano-L-proline dimers 2.26

(4) General Coupling Procedure¹⁷

(4.1) Ester Hydrolysis to Acid

Ethyl ester derivatives were hydrolyzed using LiOH (4 eq) in a 4:1 solution of MeOH/H₂O. The mixture was stirred vigorously overnight and tracked by TLC. When complete, the mixture was extracted with dichloromethane and the organic layer was disposed. The aqueous layer was acidified to pH 4 using a solution of 10% KHSO₄. The aqueous layer was then extracted with dichloromethane twice. The combined organic phase was dried over Na₂SO₄, evaporated under reduced pressure. The free acids were used in the coupling procedure without further purification.

(4.2) Boc Deprotection

N-Boc protected derivative were deprotected using TFA (10 eq) in dry dichloromethane at 0 °C. The reaction was followed by TLC (60 to 90 min). The excess TFA was neutralized with saturated sodium bicarbonate (excess). The layers were separated and the aqueous layer was extracted two times with dichloromethane (10 mL). The combined organic layers were dried over Na₂SO₄ and used directly in the coupling reaction with the activated acid, as described below. [Note: The free amine derivatives are relatively unstable as they have the tendency to attack the ester carbonyl.]

(4.3) Dimer Coupling

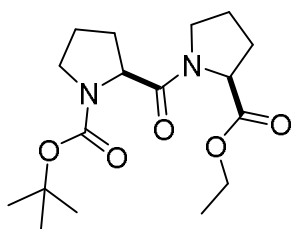
The free acid monomer was dissolved in dry dichloromethane (0.3 mM). Then, EDC.HCl (1.5 eq), HOBT (1.5), and DIPEA (4 eq) were added. The reaction was stirred at room temperature for 60 minutes. The extracted free amine was then added slowly and the mixture was left to stir overnight. The reaction was quenched with saturated NH₄Cl and the organic layer was separated, dried over Na₂SO₄ and evaporated under reduced pressure. The crude product was purified by flash chromatography (silica gel; 70% EtOAc/hexane) to afford a white solid.

pro-pro-N-Boc-L-proline dimer ethyl ester 2.23

tert-butyl (S)-2-((S)-2-(ethoxycarbonyl)pyrrolidine-1-carbonyl)pyrrolidine-1-carboxylate

Following procedure 4.1 – 300 mg of *N*-Boc-L-proline-OEt (1.2 mmol) gave 243 mg of *N*-Boc-L-proline-OH as a white solid which was then used in the procedure 4.3 for the coupling reaction. Yield = 94%.

Following procedure 4.2 and 4.3 – 300 mg of *N*-Boc-proline-OEt (1.2 mmol) was deprotected and used in the coupling reaction without purification to give 284 mg of *pro-pro-N*-Boc-L-proline dimer ethyl ester **2.23**.



Chemical Formula: C₁₇H₂₈N₂O₅
Molecular Weight: 340.42

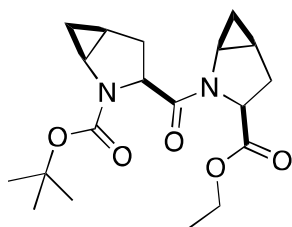
¹H NMR (400 MHz, CDCl₃, δ = 7.26) δ 4.57-4.35 ppm (m, 2H), 4.11 (m, 2H), 3.35–3.75 (m, 4H), 1.79–2.13 (m, 8H), 1.36, 1.42 (s, 9H), 1.21 (m, 3H) LC/MS: [M+Na]⁺ = 363.1742. Yield = 74%.

cis-cis-N-Boc-4,5-methano-L-proline dimer ethyl ester 2.24

tert-Butyl (1S,3S,5S)-3-((1S,3S,5S)-3-(ethoxycarbonyl)-2-azabicyclo[3.1.0]hexane-2-carbonyl)-2-azabicyclo[3.1.0]hexane-2-carboxylate

Following procedure 4.1 – 250 mg of *cis-N*-Boc-4,5-methano-L-proline-OEt **2.12** (1 mmol) gave 210 mg of *cis-N*-Boc-4,5-methano-L-proline-OH as a white solid which was then used in the procedure 4.3 for the coupling reaction. Yield = 92%.

Following procedure 4.2 and 4.3 – 250 mg of *cis-N*-Boc-4,5-methano-L-proline-OEt **2.12** (1 mmol) was deprotected and used in the coupling reaction without purification to give 160 mg of the *cis-cis-N*-Boc-4,5-methano-L-proline dimer ethyl ester **2.24**.



Chemical Formula: C₁₉H₂₈N₂O₅
Molecular Weight: 364.44

¹H NMR (500 MHz, CDCl₃, δ = 7.26) δ 5.02 (dd, J = 11.4, 3.0 Hz, 2/3H, major conformer) and 4.94 (dd, J = 11.2, 3.3 Hz, 1/3H, minor conformer), 4.83 (dd, J = 11.6, 3.3 Hz, 2/3H, major conformer) and 4.77 (dd, J = 11.6, 3.4 Hz, 1/3H, minor conformer), 4.22 – 4.00 (m, 2H), 3.54 – 3.29 (m, 2H), 2.66 – 2.46 (m, 2H), 2.32 – 2.16 (m, 1H), 2.03 – 1.91 (m, 2H), 1.82 (br s, 1H), 1.73 – 1.58 (m, 1H), 1.47 (s, 6H, major conformer) and 1.39 (s, 3H, minor conformer), 1.27 – 1.20 (m, 3H), 1.20 – 1.12 (m, 1H), 1.01 – 0.92 (m, 2H), 0.83 – 0.75 (m, 1H), 0.69 – 0.54 (m, 2H). ¹³C NMR (500 MHz, CDCl₃, δ = 77.0 ppm) δ 172.2, (172.0 minor conformer), (171.4 minor conformer), 170.9, 154.3, (153.9 minor conformer), 79.3, (60.8 minor conformer), 60.7, (60.1

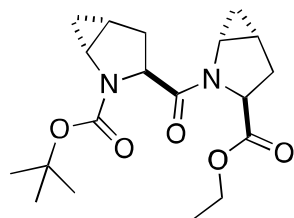
minor conformer), 59.9 minor conformer, (59.1 minor conformer), 58.6, (37.3 minor conformer), 37.1, 36.5, (30.4 minor conformer), 29.3, 29.2, 28.1, (27.9 minor conformer), 17.1, (17.0 minor conformer), 14.0, (14.0 minor conformer), 13.6, (13.3 minor conformer), 13.1, (12.4 minor conformer), 11.7. **ESI-QTOF HRMS** Calcd for C₁₉H₂₉N₂O₅ 365.2071, found 365.20772 (Error = 1.71 ppm). $[\alpha]_D^{20} = +15^\circ$ (MeOH, c = 0.6). Yield = 48%.

trans,trans- N-Boc-4,5-methano-L-proline dimer ethyl ester 2.25

tert-butyl (1R,3S,5R)-3-((1R,3S,5R)-3-(ethoxycarbonyl)-2-azabicyclo[3.1.0]hexane-2-carbonyl)-2-azabicyclo[3.1.0]hexane-2-carboxylate

Following procedure 4.1 – 250 mg of *trans-N*-Boc-4,5-methano-L-proline-COOH **2.6** (1 mmol) was esterified and used in the coupling reaction without purification.

Following procedure 4.3 – 250 mg of *trans-N*-Boc-4,5-methano-L-proline-COOH **2.6** (1.1 mmol) to give 228 mg of the *trans,trans- N*-Boc-4,5-methano-L-proline dimer ethyl ester **2.25**.



Chemical Formula: C₁₉H₂₈N₂O₅
Molecular Weight: 364.44

¹H NMR (500 MHz, CDCl₃, δ = 7.26) δ 4.65 – 4.36 (m, 2H), 4.25 – 4.06 (m, 2H), 3.58 – 3.43 (m, 1H), 3.26 – 3.14 (m, 1H), 2.50 – 2.30 (m, 2H), 2.20 (m, 2H), 1.77 (m, 1H), 1.60 (br s, 1H), 1.45 (s, 5H, major conformer),

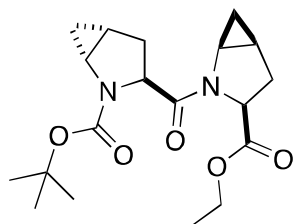
1.38 (s, 4H, minor conformer), 1.25 – 1.23 (m, 3H), 1.00 (m, 1H), 0.90 – 0.35 (m, 3H). ¹³C NMR (500 MHz, CDCl₃, δ = 77.0 ppm) δ 171.8, (171.5 minor conformer), 171.4, (171.2 minor conformer), (155.6 minor conformer), 154.9, (80.2 minor conformer), 79.7, 62.7, (61.3 minor conformer), 61.2, 60.7, (60.5 minor conformer), (60.3 minor conformer), 60.23, 38.8, (36.7 minor conformer), 36.6, (33.0 minor conformer), 32.3, (31.3 minor conformer), 31.2, 28.6, (28.4 minor conformer), (19.6 minor conformer), 19.5, 18.0, (17.7 minor conformer), (16.9 minor conformer), 16.2, (14.7 minor conformer), 14.2. **ESI-QTOF HRMS** Calcd for C₁₉H₂₉N₂O₅ (MH⁺) 365.2071, found 365.20746. [α]_D²⁰ = -221 ° (MeOH, c = 0.2). Yield = 57%.

trans-cis-N-Boc-4,5-methano-L-proline dimer ethyl ester 2.26

tert-butyl (1R,3S,5R)-3-((1S,3S,5S)-3-(ethoxycarbonyl)-2-azabicyclo[3.1.0]hexane-2-carbonyl)-2-azabicyclo[3.1.0]hexane-2-carboxylate

Following procedure 4.2 – 250 mg of *cis*-N-Boc-4,5-methano-L-proline-OEt **2.12** (1 mmol) was deprotected and used in the next step without purification.

Following procedure 4.3 – 250 mg of *trans*-N-Boc-4,5-methano-L-proline-COOH **2.6** (1.1 mmol) to give 268 mg of the *trans,cis*-N-Boc-4,5-methano-L-proline dimer ethyl ester **2.26**.



Chemical Formula: C₁₉H₂₈N₂O₅
Molecular Weight: 364.44

¹H NMR (500 MHz, CDCl₃, δ = 7.26) δ 4.88 – 4.75 (m, 1H), 4.59 (dd, *J* = 8, 6 Hz, 2/3H, major conformer), 4.47 – 4.41 (m, 1/3H, minor conformer), 4.14 (q, *J* = 7 Hz, 2H), 3.62 – 3.51 (m, 1H), 3.48 – 3.39 (m, 1H), 2.64 – 2.51 (m, 1H), 2.42 – 2.33 (m, 2H), 2.04 – 1.92 (m, 1H), 1.73 – 1.59 (m, 2H), 1.47 (s, 6H, major conformer), 1.42 (s, 3H, minor conformer), 1.25 (t, *J* = 7 Hz, 3H), 1.07 – 0.97 (m, 1H), 0.88 – 0.74 (m, 2H), 0.51 – 0.39 (m, 1H). **¹³C NMR** (500 MHz, CDCl₃, δ = 77.0 ppm) δ 172.6, (172.3 minor conformer), (170.8 minor conformer), 170.6, 155.8, (155.7 minor conformer), (80.0 minor conformer), 79.7, 61.1, (60.7 minor conformer), (60.6 minor conformer), 60.3, (59.3 minor conformer), 53.4, (38.0 minor conformer), 37.9, 36.9, (32.8 minor conformer), 32.3, 29.6, 28.4, (28.3 minor conformer), (19.4 minor conformer), 17.9, 17.2, 16.9, 16.2, (15.7 minor conformer), (14.1 minor conformer), 14.0, (13.7 major conformer). **FTIR** (cm⁻¹, ATR) ν_{max} 2976, 1743, 1697, 1664, 1400, 1185, 1133. **ESI-QTOF HRMS** Calcd for C₁₉H₂₉N₂O₅ (MH⁺) 365.2071, found 365.20843 (Error = 3.65 ppm). [α]_D²⁰ = -113 ° (CHCl₃, c = 0.8). Yield = 67%.

Diketopiperazine Formation and Analysis Procedure

(5) General Cyclization Procedure

(5.1) Boc Deprotection

N-Boc protected dimers were deprotected using trifluoroacetic acid (TFA) (10 eq) in dry dichloromethane at 0° C. The reaction was allowed to stir for approximately 60-90 min and followed by TLC. The solution was the evaporated under reduced pressure and left on a vacuum pump overnight to afford the *N*-TFA-dimer-COOEt salts.

(5.2) NMR Experiments

The *N*-TFA-dimer-COOEt salts was dissolved in DCM and the organic layer was extracted with water two times to rid of any starting material; *N*-Boc-dimer-COOEt. The combined aqueous phase was then quenched with a solution of NaHCO₃ with pH 8.5 until the pH of the aqueous phase reached 8.0-9.0 to obtain the free amine dimers. The HN-dimer-COOEt was then extracted using 0.8 mL of CDCl₃, dried over Na₂SO₄ and placed in an NMR tube. A series of ¹H NMR spectra were recorded at certain time intervals at 40 °C until completion of cyclization.

(5.3) TLC Experiments

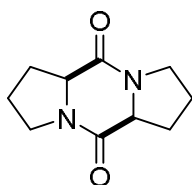
The TFA-dimer salt was dissolved in DCM. The solution was extracted in water to eliminate any remaining Boc-dimer-CO₂Et. The aqueous layer was collected and neutralized using aqueous NaHCO₃ (pH 8.5). The layers were separated and the water phase was extracted two times with DCM, dried using Na₂SO₄, and evaporated. The free amine derivatives were heated at 60 °C and DKP formation was monitored by TLC. Once the reaction was complete, the crude product was purified by flash chromatography (silica gel; MeOH/EtOAc/hexane, 1:5:4) to afford the corresponding diketopiperazine.

***pro-pro* Diketopiperazine 2.27**

(5*aS*,10*aS*)-Octahydro-5*H*,10*H*-dipyrrolo[1,2-*α*:1',2'-*d*]pyrazine-5,10-dione

Following procedure 5.1 – 100 mg of *N*-Boc-proline dimer ethyl ester **2.23** (0.3 mmol) was deprotected and used in procedure 5.2 and 5.3 to afford DKP **2.27**.

Following procedure 5.3 – 100 mg of *N*-Boc-proline dimer ethyl ester (0.3 mmol) was deprotected and cyclization was monitored by TLC at 60 °C and complete in 30 min to give 32 mg.



Chemical Formula: C₁₀H₁₄N₂O₂
Molecular Weight: 194.23

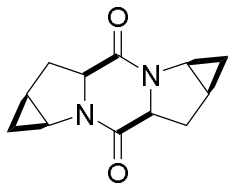
¹H NMR (500 MHz, CDCl₃ δ = 7.26) δ 4.19 (t, *J* = 8.1 Hz, 2H), 3.66-3.45 (m, 4H), 2.40-2.28 (m, 2H), 2.20 (dddd, *J* = 13.0, 10.6, 9.2, 7.2 Hz 2H), 2.11-1.99 (m, 2H), 1.99-1.86 (m, 2H). ¹³C NMR (500 MHz, CDCl₃ δ = 77.0 ppm) δ 166.3, 60.5, 45.2 27.6, 23.3. **ESI-QTOF HRMS** Calcd for C₁₀H₁₅N₂O₂ 195.1128, found 195.1128 (Error = -1.82 ppm). Yield = 55%.

***cis-cis* Diketopiperazine 2.28**

(1*aS*,3*aS*,4*aS*,5*aS*,7*aS*,8*aS*)-Octahydrocyclopropa[4,5]pyrrolo[1,2-*α*]cyclopropa[4,5]pyrrolo [1,2-*d*]pyrazine-3,7(1*H*,3*aH*)-dione

Following procedure 5.1 – 100 mg of *cis,cis*- *N*-Boc-4,5-methano-L-proline dimer ethyl ester **2.24** (0.27 mmol) was deprotected and used in procedure 5.2 and 5.3 to afford the *cis-cis* DKP **2.28**.

Following procedure 5.3 - 100 mg of *cis,cis*- *N*-Boc-4,5-methano-L-proline dimer ethyl ester (0.27 mmol) was deprotected and cyclization was monitored by TLC at 60 °C and complete in 5 h to give 24 mg.



Chemical Formula: $C_{12}H_{14}N_2O_2$
Molecular Weight: 218.26

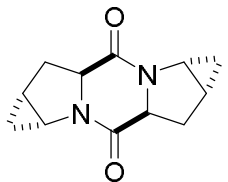
1H NMR (500 MHz, $CDCl_3$ $\delta = 7.26$) δ 4.67 (dd, $J = 9, 7$ Hz, 2H), 3.48 (td, $J = 6, 2$ Hz, 2H), 2.58 (ddd, $J = 14, 10, 7$ Hz, 2H), 2.45 (ddd, $J = 14, 7, 2$ Hz, 2H), 1.78 – 1.66 (m, 2H), 1.10 (dt, $J = 9, 5$ Hz, 2H), 0.46 – 0.33 (m, 2H). ^{13}C NMR (500 MHz, $CDCl_3$ $\delta = 77.0$ ppm) δ 167.2, 65.0, 37.1, 29.6, 20.6, 15.9. FTIR (cm^{-1} , ATR) ν_{max} 3061, 2955, 1661, 1397, 806, 750. ESI-QTOF HRMS Calcd for $C_{12}H_{15}N_2O_2$ 219.1128, found 219.11296 (Error = 0.73 ppm). $[\alpha]_D^{20} = 35^\circ$ ($CDCl_3$, $c = 9$). Yield = 40%.

trans-trans Diketopiperazine 2.29

(1*aR*,3*aS*,4*aR*,5*aR*,7*aS*,8*aR*)-Octahydrocyclopropa[4,5]pyrrolo[1,2-*d*]cyclopropa[4,5]pyrrolo [1,2-*d*]pyrazine-3,7(1*H*,3*aH*)-dione

Following procedure 5.1 – 100 mg of *trans,trans*- *N*-Boc-4,5-methano-L-proline dimer ethyl ester **2.25** (0.27 mmol) was deprotected and used in procedure 5.2 and 5.3 to afford the *trans-trans* DKP **2.29**.

Following procedure 5.3 – 100 mg of *trans,trans*- *N*-Boc-4,5-methano-L-proline dimer ethyl ester (0.27 mmol) was deprotected and cyclization was monitored by TLC at 60 °C and complete in 1 h to give 34 mg.



Chemical Formula: $C_{12}H_{14}N_2O_2$
Molecular Weight: 218.26

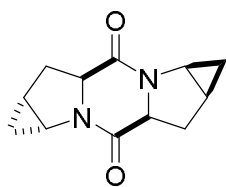
¹H NMR (500 MHz, CDCl₃ δ = 7.26) δ 3.89 (dd, *J* = 13.6, 5 Hz, 2H), 3.84 (td, *J* = 6.3, 2.5 Hz, 2H), 2.47-2.34 (m, 4H), 1.64 (dt, *J* = 11, 5.2 Hz 2H), 0.84 (dtd, *J* = 8.6, 6.4, 0.9 Hz, 2H), 0.69-0.64 (m, 2H). ¹³C NMR (500 MHz, CDCl₃ δ = 77.0 ppm) δ 165.7, 56.9, 34.3, 29.6, 12.9, 8.8. FTIR (cm⁻¹, ATR) ν_{max} 1662, 1435, 1203. ESI-QTOF HRMS Calcd for C₁₂H₁₅N₂O₂ 219.1128, found 219.1126 (Error = -0.82ppm). [α]_D²⁰ = -96 ° (CDCl₃, c = 9). Yield = 56%.

trans-cis Diketopiperazine **2.30**

(1*aR*,3*aS*,4*aS*,5*aS*,7*aS*,8*aR*)-Octahydrocyclopropa[4,5]pyrrolo[1,2-*a*]cyclopropa[4,5]pyrrolo [1,2-*d*]pyrazine-3,7(1*H*,3*aH*)-dione

Following procedure 5.1 – 100 mg of *trans,cis*- *N*-Boc-4,5-methano-L-proline dimer ethyl ester **2.26** (0.27 mmol) was deprotected and used in procedure 5.2 and 5.3 to afford the *trans-cis* DKP **2.30**.

Following procedure 5.3 – 100 mg of of *trans,cis*- *N*-Boc-4,5-methano-L-proline dimer ethyl ester (0.27 mmol) was deprotected and cyclization was monitored by TLC at 60 °C and complete in 3 h to give 21 mg.



Chemical Formula: C₁₂H₁₄N₂O₂
Molecular Weight: 218.26

¹H NMR (500 MHz, CDCl₃ δ = 7.26) δ 4.72 (ddd, *J* = 9.9, 8.5, 1.7 Hz, 1H), 3.90-3.79 (m, 2H), 3.46 (m, 1H), 2.63 (ddd, *J* = 13.2, 8.9, 7.3 Hz 1H), 2.51-2.36 (m, 2H), 2.27 (ddd, *J* = 13.9, 8.3, 1.9 Hz 1H), 1.72 (m, 1H), 1.63 (ddd, *J* = 11, 8.7, 5.4 Hz, 1H), 1.13 (m, 1H), 0.84 (m, 1H), 0.61 (m, 1H), 0.49 (m, 1H). ¹³C NMR (500 MHz, CDCl₃ δ = 77.0 ppm) δ 166.4, 165.9, 66.2, 57.0, 37.0, 34.6, 30.7, 29.2, 21.4, 15.5, 13.4, 9.85. FTIR (cm⁻¹, ATR) ν_{max} 2921, 1662.4, 1433.0. ESI-QTOF HRMS Calcd for C₁₂H₁₅N₂O₂ 219.1128, found 219.1128 (Error = -0.16 ppm). [α]_D²⁰ = -44° (CDCl₃, c = 5). Yield = 36%.

References

1. Perez-Arellano, I.; Carmona-Alvarez, F.; Martinez, A. I.; Rodriguez-Diaz, J.; Cervera, J., Pyrroline-5-carboxylate synthase and proline biosynthesis: from osmotolerance to rare metabolic disease. *Protein Sci* **2010**, *19* (3), 372-82.
2. Graupner, M.; White, R. H., Methanococcus jannaschii generates L-proline by cyclization of L-ornithine. *J Bacteriol* **2001**, *183* (17), 5203-5.
3. (a) Notz, W.; Tanaka, F.; Barbas, C. F., 3rd, Enamine-based organocatalysis with proline and diamines: the development of direct catalytic asymmetric Aldol, Mannich, Michael, and Diels-alder reactions. *Acc Chem Res* **2004**, *37* (8), 580-91; (b) Enders, D.; Gasperi, T., Proline organocatalysis as a new tool for the asymmetric synthesis of ulosonic acid precursors. *Chem Commun (Camb)* **2007**, (1), 88-90; (c) Yang, H.; Carter, R. G., Proline Sulfonamide-Based Organocatalysis: Better Late than Never. *Synlett* **2010**, *2010* (19), 2827-2838.
4. Shoulders, M. D.; Raines, R. T., Collagen structure and stability. *Annu Rev Biochem* **2009**, *78*, 929-58.
5. Horng, J. C.; Raines, R. T., Stereoelectronic effects on polyproline conformation. *Protein Sci* **2006**, *15* (1), 74-83.
6. DeRider, M. L.; Wilkens, S. J.; Waddell, M. J.; Bretscher, L. E.; Weinhold, F.; Raines, R. T.; Markley, J. L., Collagen stability: insights from NMR spectroscopic and hybrid density functional computational investigations of the effect of electronegative substituents on prolyl ring conformations. *J Am Chem Soc* **2002**, *124* (11), 2497-505.
7. Panasik, N., Jr.; Eberhardt, E. S.; Edison, A. S.; Powell, D. R.; Raines, R. T., Inductive effects on the structure of proline residues. *Int J Pept Protein Res* **1994**, *44* (3), 262-9.
8. Improta, R.; Benzi, C.; Barone, V., Understanding the role of stereoelectronic effects in determining collagen stability. 1. A quantum mechanical study of proline, hydroxyproline, and fluoroproline dipeptide analogues in aqueous solution. *J Am Chem Soc* **2001**, *123* (50), 12568-77.
9. *Protein Stability and Folding: Theory and Practice*. Humana Press Inc.: Totowa, NJ, 1995; Vol. 40.
10. Adzhubei, A. A.; Sternberg, M. J.; Makarov, A. A., Polyproline-II helix in proteins: structure and function. *J Mol Biol* **2013**, *425* (12), 2100-32.
11. S. Hanessian, U. R., G. Gentile. The Synthesis of Enantiopure ω -Methanoprolines and ω -Methanopipicolinic Acids by a Novel Cyclopropanation Reaction: The "Flattering" of Proline. *Angew. Chem. Int. Ed. Engl.* **1997**, *36* (17), 1881-1884.
12. Dong, J.; Gong, Y.; Liu, J.; Chen, X.; Wen, X.; Sun, H., Synthesis and biological evaluation of all eight stereoisomers of DPP-IV inhibitor saxagliptin. *Bioorg Med Chem* **2014**, *22* (4), 1383-93.
13. Magnin, D. R.; Robl, J. A.; Sulsky, R. B.; Augeri, D. J.; Huang, Y.; Simpkins, L. M.; Taunk, P. C.; Betebenner, D. A.; Robertson, J. G.; Abboa-Offei, B. E.; Wang, A.; Cap, M.; Xin, L.; Tao, L.; Sitkoff, D. F.; Malley, M. F.; Gougoutas, J. Z.; Khanna, A.; Huang, Q.; Han, S. P.; Parker, R. A.; Hamann, L. G., Synthesis of novel potent dipeptidyl peptidase IV inhibitors with enhanced chemical stability: interplay between the N-terminal amino acid alkyl side chain and the cyclopropyl group of alpha-aminoacyl-L-cis-4,5-methanoprolinenitrile-based inhibitors. *J Med Chem* **2004**, *47* (10), 2587-98.
14. Wilhelm, P.; Lewandowski, B.; Trapp, N.; Wennemers, H., A crystal structure of an oligoproline PPII-helix, at last. *J Am Chem Soc* **2014**, *136* (45), 15829-32.
15. Benedetti, E. B., A.; di Blasio, B.; Pavone, V.; Pedone, C.; Toniolo, C. B., G. M., Solid-State Geometry and Conformation of Linear, Diastereoisomeric Oligoprolines. *Biopolymers* *22*, 305-317.
16. Vitagliano, L.; Berisio, R.; Mastrangelo, A.; Mazzarella, L.; Zagari, A., Preferred proline puckerings in cis and trans peptide groups: implications for collagen stability. *Protein Sci* **2001**, *10* (12), 2627-32.

17. Berger, G.; Vilchis-Reyes, M.; Hanessian, S., Structural Properties and Stereochemically Distinct Folding Preferences of 4,5-cis and trans-Methano-L-Proline Oligomers: The Shortest Crystalline PPII-Type Helical Proline-Derived Tetramer. *Angew Chem Int Ed Engl* **2015**, *54* (45), 13268-72.
18. Hinderaker, M. P.; Raines, R. T., An electronic effect on protein structure. *Protein Sci* **2003**, *12* (6), 1188-94.
19. Kuemin, M.; Nagel, Y. A.; Schweizer, S.; Monnard, F. W.; Ochsenfeld, C.; Wennemers, H., Tuning the cis/trans conformer ratio of Xaa-Pro amide bonds by intramolecular hydrogen bonds: the effect on PPII helix stability. *Angew Chem Int Ed Engl* **2010**, *49* (36), 6324-7.
20. Siebler, C.; Maryasin, B.; Kuemin, M.; Erdmann, R. S.; Rigling, C.; Grünenfelder, C.; Ochsenfeld, C.; Wennemers, H., Importance of dipole moments and ambient polarity for the conformation of Xaa-Pro moieties – a combined experimental and theoretical study. *Chem. Sci.* **2015**, *6* (12), 6725-6730.
21. Enrique Pedroso, A. G., Xavier de las Heras, Ramon Eritja and Ernest Giralt, Diketopiperazine Formation in Solid Phase Peptide Synthesis Using p-Alkoxybenzyl Ester Resins and Fmoc-Amino Acids. *Tetrahedron Letters* **1986**, *27* (6), 743-746.
22. Curran, T. P.; Marcaurelle, L. A.; O'Sullivan, K. M., A short synthesis of bicyclic dipeptides corresponding to Xxx-L-Pro Xxx-D-Pro having constrained trans-proline amides. *Org Lett* **1999**, *1* (8), 1225-8.
23. Goolcharran, C.; Borchardt, R. T., Kinetics of diketopiperazine formation using model peptides. *J Pharm Sci* **1998**, *87* (3), 283-8.
24. Larsen, S. W.; Ankersen, M.; Larsen, C., Kinetics of degradation and oil solubility of ester prodrugs of a model dipeptide (Gly-Phe). *Eur J Pharm Sci* **2004**, *22* (5), 399-408.
25. Brackmann, F.; Colombo, N.; Cabrele, C.; de Meijere, A., An Improved Synthesis of 3,4-(Aminomethano)proline and Its Incorporation into Small Oligopeptides. *European Journal of Organic Chemistry* **2006**, *2006* (19), 4440-4450.
26. Hanessian, S.; Reinhold, U.; Saulnier, M.; Claridge, S., Probing the importance of spacial and conformational domains in captopril analogs for angiotensin converting enzyme activity. *Bioorg Med Chem Lett* **1998**, *8* (16), 2123-8.
27. Wang, G.; James, C. A.; Meanwell, N. A.; Hamann, L. G.; Belema, M., A scalable synthesis of (1R,3S,5R)-2-(tert-butoxycarbonyl)-2-azabicyclo[3.1.0]hexane-3-carboxylic acid. *Tetrahedron Letters* **2013**, *54* (49), 6722-6724.
28. Berger, G.; Chab-Majdalani, I.; Hanessian, S., Properties of the amide bond involving proline 4,5-methanologues: an experimental and theoretical study. *Israel Journal of Chemistry* **2016**.
29. Miyashita, K.; Murakami, M.; Yamada, M.; Iriuchijima, T.; Mori, M., Histidyl-proline diketopiperazine. Novel formation that does not originate from thyrotropin-releasing hormone. *J Biol Chem* **1993**, *268* (28), 20863-5.
30. (a) Wennemers, H.; Nold, M. C.; Conza, M. M.; Kulicke, K. J.; Neuburger, M., Flexible but with a defined turn-influence of the template on the binding properties of two-armed receptors. *Chemistry* **2003**, *9* (2), 442-8; (b) Wennemers, H.; Sonntag, L.-S.; Ivan, S.; Langer, M.; Conza, M. M., Functionalized Cyclotriproline - A Bowl-Shaped Tripodal Scaffold. *Synlett* **2004**, (7), 1270-1272; (c) Sonntag, L. S.; Schweizer, S.; Ochsenfeld, C.; Wennemers, H., The "azido gauche effect"-implications for the conformation of azidoproline. *J Am Chem Soc* **2006**, *128* (45), 14697-703.
31. Abe, M.; Imai, T.; Ishii, N.; Usui, M., Synthesis of quinolactamide via an acyl migration reaction and dehydrogenation with manganese dioxide, and its insecticidal activities. *Biosci Biotechnol Biochem* **2006**, *70* (1), 303-6.

